AD-A179 253 RESILIENT MODULUS OF FREEZE-THAW AFFECTED GRANULAR SOILS FOR PAVEMENT DES..(U) COLD REGIONS RESEARCH AND ENGINEERING LAB HANOVER NH D M COLE ET AL. FEB 87 1/1

UNCLASSIFIED CRREL-87-2 DOT/FAA/PM-84-16-PT-3 F/G 8/13 NL

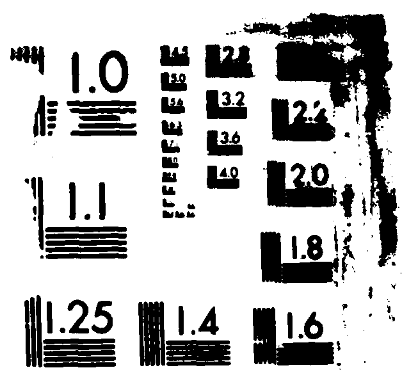

MI

2

DOT/FAA/PM-84/16,3

Program Engineering
and Maintenance Service
Washington, D.C. 20591

Resilient Modulus of Freeze-Thaw Affected Granular Soils for Pavement Design and Evaluation

Part 3. Laboratory Tests on Soils from Albany County Airport

D.M. Cole
D.L. Bentley
G.D. Durell
T.C. Johnson

U.S. Army Cold Regions Research and
Engineering Laboratory
Hanover, New Hampshire 03755-1290

February 1987

This document is available to the public
through the National Technical Information
Service, Springfield, Virginia 22161

U.S. Department of Transportation
Federal Aviation Administration

For conversion of SI metric units to U.S./British customary units of measurement consult ASTM Standard E380, Metric Practice Guide, *published by the American Society for Testing and Materials, 1916 Race St., Philadelphia, Pa. 19103.*

NOTICE

Technical Report Documentation Page

1. Report No. DOT/FAA/PM-84/16,3	2. Government Accession No. A179253	3. Recipient's Catalog No.
4. Title and Subtitle RESILIENT MODULUS OF FREEZE-THAW AFFECTED GRANULAR SOILS FOR PAVEMENT DESIGN AND EVALUATION. Part 3. Laboratory Tests on Soils from Albany County Airport		5. Report Date February 1987
		6. Performing Organization Code
7. Author(s) D.M. Cole, D.L. Bentley, G.D. Durell and T.C. Johnson		8. Performing Organization Report No. CRREL Report 87-2
9. Performing Organization Name and Address U.S. Army Cold Regions Research and Engineering Laboratory Hanover, New Hampshire 03755-1290		10. Work Unit No. (TRAIS)
		11. Contract or Grant No. FHWA-8-3-0187
12. Sponsoring Agency Name and Address U.S. Department of Transportation Federal Aviation Administration Program Engineering and Maintenance Service Washington, D.C. 20591		13. Type of Report and Period Covered
		14. Sponsoring Agency Code APM-740

15. Supplementary Notes

Co-sponsored by: Federal Highway Administration, Washington, D.C.
Office of the Chief of Engineers, U.S. Army, Washington, D.C.

16. Abstract

This is the third in a series of four reports on the laboratory and field testing of a number of road and airfield subgrades, covering the laboratory repeated-load triaxial testing of five soils in the frozen and thawed states and analysis of the resulting resilient modulus measurements. The laboratory testing procedures allow simulation of the gradual increase in stiffness found in frost-susceptible soils after thawing. The resilient modulus is expressed in a nonlinear model in terms of the applied stresses, the soil moisture tension level (for unfrozen soil), the unfrozen water content (for frozen soil) and the dry density. The resilient modulus is about 10 GPa for the frozen material at temperatures in the range of -5° to -8°C. The decrease in modulus with increasing temperature was well-modeled in terms of the unfrozen water content. Upon thaw, the modulus dropped to about 100 MPa and generally increased with increasing confining stress and decreased with increasing principal stress ratio. The modulus also increased with the soil moisture tension level. The resilient Poisson's ratio did not appear to be a systematic function of any of the test variables.

17. Key Words Airfields, Freezing-thawing, Laboratory tests, Repeated-load triaxial tests, Resilient moduli, Roads, Soil tests, Subgrade soils	18. Distribution Statement This document is available to the public through the National Technical Information Service, Springfield, Virginia 22161.

19. Security Classif. (of this report)	20. Security Classif. (of this page)	21. No. of Pages	22. Price
Unclassified	Unclassified	40	

Form DOT F 1700.7 (8-72) Reproduction of completed page authorized

(A)

PREFACE

This report was prepared by David M. Cole, Research Civil Engineer, Applied Research Branch, Experimental Engineering Division; Diane L. Bentley, Research Civil Engineer, Civil Engineering Research Branch, Experimental Engineering Division; Glenn D. Durell, Mechanical Engineering Technician, Engineering and Measurement Services Branch, Technical Services Division, and Thaddeus C. Johnson, Civil Engineer and Chief of the Civil Engineering Research Branch, Experimental Engineering Division, U.S. Army Cold Regions Research and Engineering Laboratory.

This report covers certain aspects of a project partially funded by the Federal Highway Administration and the Federal Aviation Administration, and the Office of the Chief of Engineers through DA Project 4A762730AT42, *Design, Construction and Operations Technology for Cold Regions;* Task A2, *Soils and Foundations Technology/Cold Regions;* Work Unit 004, *Seasonal Change in Strength and Stiffness of Soils and Base Courses.*

The work was done at CRREL and a number of people contributed to the successful conclusion of this area of the project. The authors acknowledge in particular E. Chamberlain who was closely involved in equipment development, D. Carbee for his help in specimen preparation, D. Keller who assisted in field coring and sample preparation, L. Irwin for helpful discussions of the test results, J. Ingersoll who was responsible for generating the moisture characteristic curves and who assisted in the development of the tensiometer systems, and A. Tice who generated the unfrozen water content data for the test soils.

This report was technically reviewed by E.J. Chamberlain and F. Sayles of CRREL.

The contents of this report are not to be used for advertising or promotional purposes. Citation of brand names does not constitute an official endorsement or approval of the use of such commercial products.

CONTENTS

ILLUSTRATIONS

TABLES

Resilient Modulus of Freeze–Thaw Affected Granular Soils for Pavement Design and Evaluation

Part 3. Laboratory Tests on Soils from Albany County Airport

D.M. COLE, D.L. BENTLEY, G.D. DURELL AND T.C. JOHNSON

INTRODUCTION

This is one of four reports that document the laboratory and field test results of an extensive research effort jointly funded by the U.S. Army Corps of Engineers, the Federal Highway Administration and the Federal Aviation Administration. The project, entitled *Full-Scale Field Tests to Evaluate Frost Action Predictive Techniques*, called for laboratory testing and field verification of the resilient properties of a number of test soils located at Winchendon, Massachusetts (the subject of Parts 1 and 2 [Cole et al. 1986, Johnson et al. 1986a] of this series of reports) and Albany, New York (the subject of this report and Part 4 [Johnson et al. 1986b]). Part 1 includes detailed descriptions of the laboratory testing procedures and methods of data analysis and interpretation. Consequently, this report does not dwell on such matters, but instead concentrates on the presentation and analysis of results from the two taxiways that we investigated at the Albany County Airport.

The objectives of the work call for characterizing the test soils under a variety of seasonal conditions: frozen, thawed and recovered. The first two conditions are self-explanatory; "recovered" refers to soil that has drained and possibly consolidated after thawing and has consequently regained (or recovered) the same degree of stiffness it possessed prior to the freezing and thawing cycle. The testing sequence used in the laboratory work is designed to simulate the progression of events that the soils experience in the field. This process relies heavily on the use of soil moisture tension and temperature as links between laboratory and field results.

Part 4 (Johnson et al. 1986b), the companion to this report, presents the results of the surface deflection measurements on the two taxiways and verifies the laboratory-determined resilient modulus expressions developed in the present work. The verification is accomplished through the use of a computer code (called NELAPAV) that carries out a layered elastic analysis of the pavement system. The program and the verification procedure have been covered in detail elsewhere (Irwin and Johnson 1981).

Field data on the temperature and moisture tension history of the test sections provided the appropriate range of these variables in the laboratory testing. Specimens were first tested in repeated-load triaxial compression in the frozen state, beginning with the lowest temperature, at several values of axial stress and a single value (69.0 kPa) of confining stress. Next, the specimens were completely thawed on specially designed triaxial cell bases (see Cole et al. 1986) and tested at up to five levels of soil moisture tension. The increases in moisture tension were achieved by drawing water from the specimen via the triaxial cell's drainage system. This procedure simulates the gradual recovery of stiffness experienced by thaw-weakened soils.

The repeated-load triaxial testing yields the resilient modulus, M_r (defined as cyclic stress divided by recoverable axial strain), as a function of applied stresses, temperature (for soils in the frozen state), moisture tension ψ (for the unfrozen state), and dry unit weight γ_d where applicable. A simple nonlinear relationship of the form

$$M_r = k_1[f(\sigma)]^{k_2} \tag{1}$$

is used to represent the test data—k_1 is generally a function of ψ, and in some cases γ_d, and k_2 is a constant. A linear regression technique is used to find constants that give the best fit to the test data.

The stress function $f(\sigma)$ is taken as either the commonly used first stress invariant J_1 (sum of the principal stresses) or the ratio J_2/τ_{oct} (ratio of the second stress invariant to the octahedral shear stress). The latter function has been examined at length by Cole et al. (1981, 1986). Its usefulness stems from its ability to adequately reflect the tendency of many granular soils to exhibit an increasing modulus with both increasing confining stress (σ_3) and decreasing principal stress ratio (σ_1/σ_3). All analyses are carried out in terms of both stress functions for comparison.

The reader is referred to Cole et al. (1986) for extensive background information on the project in general as well as for details of the laboratory testing methodology. The Albany County Airport work closely follows the Winchendon, Massachusetts, activity with one exception: we tested no field cores from the Albany site. All specimens were remolded in the laboratory using material that had been remixed according to the original gradation specifications for the taxiway sections.

TEST SECTIONS AND MATERIALS

Figure 1 gives cross sections of each taxiway. Field instrumentation yielded temperature and moisture tension profiles for each section, which are presented by Johnson et al. (1986b). Gradation curves for the test soils appear in Figure 2, and Table 1 gives some physical characteristics and classifications for the soils.

The water table fluctuated seasonally between 1.5 and 2.0 m at both sites. Frost penetration depths for the periods of observation are given by Johnson et al. (1986b).

Taxiway A consists of a layer of asphalt concrete, a crushed stone base, a gravelly sand subbase and a silty fine sand subgrade. Taxiway B consists of a badly broken layer of asphalt concrete, an asphalt penetration macadam stone base, a silty sandy gravel subbase and a silty fine sand subgrade.

Since the moisture retention characteristics of these materials are of interest, the moisture tension versus water content curves were determined for several of the soils in the laboratory. Curves for the Taxiway A base and subbase and the Taxiway B subgrade appear in Appendix A. The subgrades for both taxiways were nearly identical, so the Taxiway B subgrade curve is assumed valid for Taxiway A as well. We were not able to obtain such data for the Taxiway B subbase since it was too coarse to test in our cell.

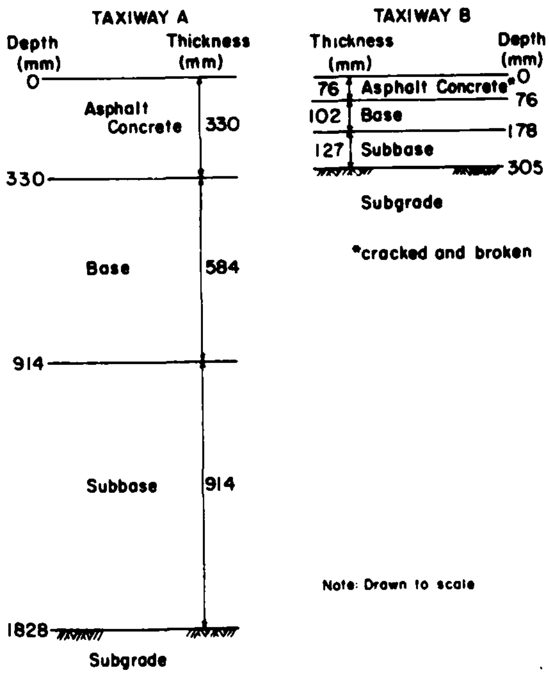

Figure 1. Albany Airport taxiway profiles.

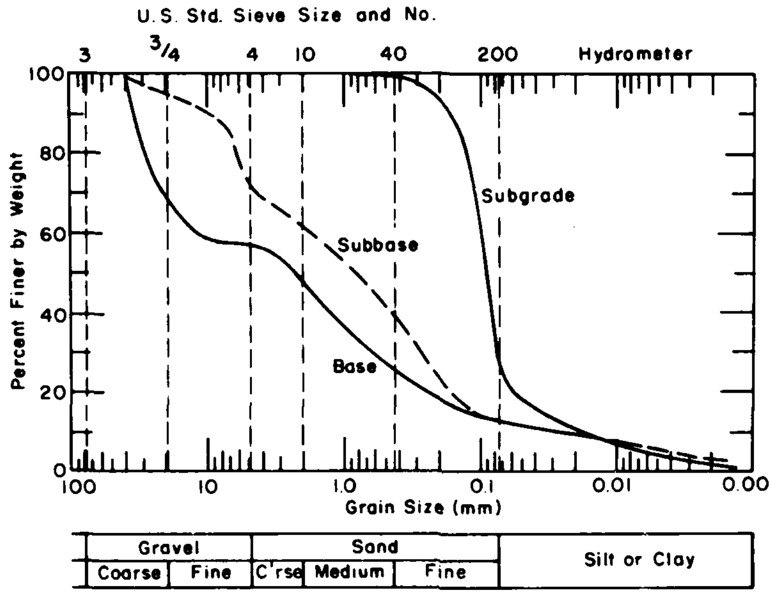

a. Taxiway A.

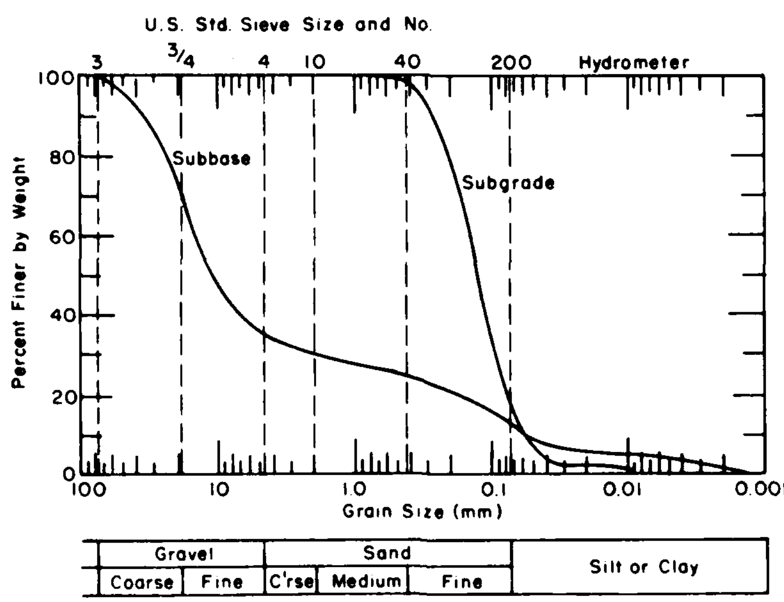

b. Taxiway B.

Figure 2. Gradation curves for Albany soils.

Table 1. Physical characteristics and classification of the Albany Airport soils.

Soil	Unified Soil Classification	Maximum size (mm)	Coefficients C_u	C_c	Specific gravity
Taxiway A subbase	SM	19.1	95.8	2.2	2.73
Taxiway A subgrade	SM	0.42	4.0	1.6	2.67
Taxiway B subbase	GM	19.1	16.3	0.22	2.68
Taxiway B subgrade	SM	0.42	2.7	1.2	2.69

SPECIMEN PREPARATION

Test soils

We obtained shovel samples of all the layers of material. Since it was impossible to distinguish between the base and subbase materials of Taxiway B because of the deterioration and insufficient thickness of the base, both layers were sampled and tested as a single material.

The various soils were sieved and remixed in the laboratory according to original specifications. The coarse-grained materials were compacted in a 152-mm-diameter, 305-mm-high mold and were frozen at a rate of 25 mm/day under open system conditions. These specimens were capped in the manner described by Cole et al. (1986). They did not heave appreciably (i.e., less than 10% of specimen height). The fine-grained subgrade material was compacted in a tapered 152-mm-diameter, 152-mm-high mold and subjected to the same freezing conditions. Once the material was frozen, several 51-mm-diameter, 127-mm-long specimens were machined from the samples and carefully trimmed prior to testing.

Since the frost did not penetrate to the depth of interest insofar as the layered elastic analysis was concerned, it was necessary to characterize the subgrade in the unfrozen (as well as frozen and thawed) state. For this purpose, specimens (51 mm in diameter by 127 mm long) were merely compacted to design specifications and tested.

Additional details of the preparation procedures are given by Cole et al. (1986).

Asphalt concrete

We were able to obtain usable cores of the asphalt concrete layers for both taxiways. Taxiway A was sufficiently thick to yield 102-mm-diameter, 250-mm-long cores, which were easily trimmed and tested. The thin asphalt layer of Taxiway B, however, made it necessary for us to form a specimen of adequate height by stacking three of the short cores and binding them together with a thin layer of asphalt emulsion. The asphalt concrete was tested in the dry state, although moisture content is expected to affect the resilient behavior (Johnson et al. 1978).

LABORATORY TESTING

All testing of the soils was carried out in one of two triaxial cells, depending upon specimen size. The asphalt concrete was tested only in uniaxial compression. For all laboratory tests, we used an electro-hydraulic, closed-loop testing machine operated in LOAD control.

To achieve a steady-state response, 200 loading cycles were applied at each combination of axial and radial stress. The M_r values were calculated from a representative cycle near the end of each run.

The test equipment and procedures are fully described by Cole et al. (1986).

Soil testing

Two triaxial cells, with several unique features, were designed and built for this testing program. The cells differed primarily in size: one accommodated the 51-mm-diameter specimens while the other accommodated the 152-mm-diameter specimens. The cells featured removable bases, which facilitated the sequential testing of each specimen, and built-in tensiometer systems to continuously monitor soil moisture tension.

Since handling of the frozen specimens presented no serious problems given adequate coldroom facilities, a single cell base equipped with a thermocouple was used for the frozen state tests. However, since many specimens were often extremely weak and deformable upon thawing, the removable cell base concept was developed. This approach called for designing triaxial cells that could be completely assembled about a specimen that was mounted on the cell base. We used up to six bases for the small cell and four for the large cell. In this manner, a number of specimens could be tested sequentially without removing them from their respective cell bases. The major cell components and the deformation and load measuring devices were easily transferred from one base to another. Cole et al. (1986) give details of this procedure and of the equipment design.

The sequential testing approach was used to allow the maximum amount of testing on each specimen and to allow use of the major cell components while tested specimens were equilibrating at new moisture tension levels. Simulation of the recovery period after thawing was achieved by alternately testing and drying each specimen until the moisture tension reached the level observed in the field. At each level of moisture tension, a specimen was subjected to the sequence of confining and nominal deviator stresses given in Cole et al. (1986). The actual deviator stresses at each data point, with slight corrections for the changes in specimen area, are given in Appendix B. All of the triaxial tests were carried out with a vacuum applied to the specimen through the drainage system. The vacuum level coincided with the desired soil moisture tension level for the test. This was done to ensure a constant moisture tension level throughout load cycling.

Axial deformation was measured on the specimen with a system of four Linear Variable Differential Transformers (LVDTs), which measured the relative displacement of two circumferentially mounted rings. Radial displacement was measured at three points, equally spaced about the circumference, at midheight on the specimen. The load was monitored by a miniature load cell, mounted in the triaxial cell, in direct contact with the top cap of the specimen. This load cell also served as a feedback, controlling the load applied by the testing machine.

These measurements allowed the calculation of both resilient and permanent strains in the axial and radial directions, which in turn allowed the calculation of resilient modulus and resilient Poisson's ratio (μ_r).

Waveforms of applied stress

The soils were subjected to two loading waveforms that correspond to the loading characteristics of the two devices used in the surface deflection tests done in the field. The waveform simulating the Repeated-load Plate-Bearing apparatus (designated RPB) was a 1-s-on, 2-s-off pulse. A 28-ms haversine, repeated every 2 s was used to simulate the load pulse produced by the Falling-Weight Deflectometer (designated FWD) (Fig. 3).

Throughout the course of this study, we made a gradual shift in the field verification work from the use of the RPB device to the FWD device. In the Albany County Airport work, we used the FWD device exclusively, but continued to apply the RPB loading waveform in the laboratory testing for the sake of continuity with earlier work.

Initial tests indicated that there was no significant difference in the modulus determined with these two waveforms, so we decided to apply the FWD pulse as a rule and spot-check the modulus

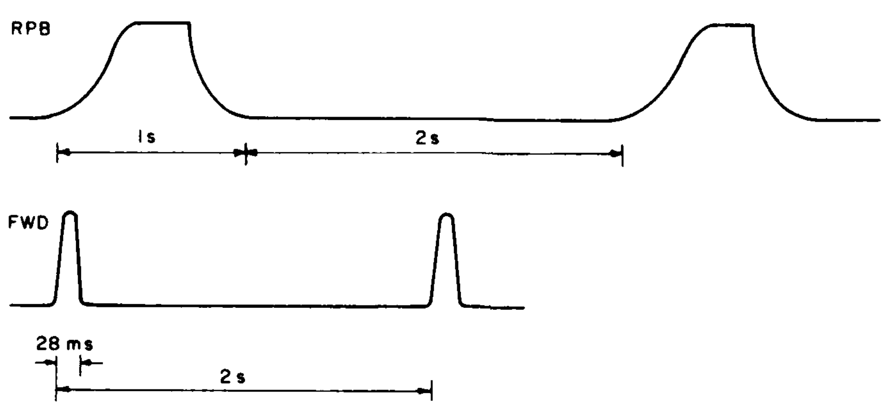

Figure 3. Load pulse waveforms used in the repeated load triaxial tests (repeated load plate-bearing apparatus [RPB] waveform and falling-weight deflectometer [FWD] waveform).

periodically with the RPB pulse. Consequently, in contrast to Cole et al. (1986) where modulus equations were presented for each waveform separately, the equations presented in this work are applicable to both waveforms for all granular materials.

Asphalt concrete

The asphalt concrete cores were tested at temperatures of -10°, 5°, 25° and 40°C in uniaxial compression. Maximum axial cyclic stresses of approximately 68.0, 103.0, 136.0, 174.0 and 228.0 kPa were applied under three waveforms.

Axial deformation was measured using LVDTs mounted on circumferential clamps. Load was measured by a load cell mounted on the actuator of the testing machine. The machine was operated in LOAD control, as in the soil tests.

The asphalt concrete tests employed three waveforms: the RPB and FWD pulses described earlier and a continuous haversine at frequencies of 1, 4 and 16 Hz. The latter loading condition was included for completeness and is according to ASTM D3497-79T (ASTM 1981).

DATA REDUCTION AND ANALYSIS

Soil

The frozen state test on a given soil yields an M_r value for a certain stress level and temperature. Testing in the thawed or unfrozen states yields an M_r value for a given applied stress state and moisture tension level. Not all of the stress levels given in Cole et al. (1986) could be applied to each specimen at all values of moisture tension, ψ. Since each specimen was tested a number of times, it was important to avoid excessive permanent deformation in the early stages of testing. Consequently, the testing of thawed material at low ψ values was often terminated before the higher stress levels were applied. Appendix B gives the actual stress levels applied for each test. In general, newly thawed specimens (ψ = 2 kPa) were tested to deviator and confining stress levels of approximately 28 kPa; the associated resilient axial strains were approximately 3×10^{-4} to 4×10^{-4}. Stiffer specimens were tested to stress levels of approximately 70 kPa and corresponding strain levels near 8×10^{-4}.

As a result of the testing sequence, each specimen generated from 50 to 70 data points. Each of these data points represents a nominally steady state material response after 200 load cycles. The resilient behavior generally stabilized within 10–20 cycles for the lower stress levels and within about 50 cycles for the higher stress levels.

The test data were subjected to multiple linear regression analysis, the details of which are given in Cole et al. (1986). We employed the simple nonlinear expression given by eq 1 to represent the material in the thawed state. The coefficient k_1 was treated as a function of ψ and γ_d, where applicable. The exponent k_2 was considered constant for a given material with a given freeze–thaw history. Earlier work indicated that k_2 does not vary systematically with ψ (Cole et al. 1981).

The analyses employ one of two stress functions to model the stress dependency of the thawed soils: J_1 the first stress invariant, and J_2/τ_{oct}, the second stress invariant divided by the octahedral shear stress. The former stress function is traditional and reflects the tendency of the modulus to increase with increasing bulk stress. However, J_1 is insensitive to the effect of the principal stress ratio σ_1/σ_3. It is frequently observed for granular soils that modulus decreases as the principal stress ratio increases. The latter stress function, J_2/τ_{oct}, addresses the effect of principal stress ratio and thus proves useful in the present analysis.

In a common repeated-load triaxial test, where $\sigma_2 = \sigma_3$ and $\sigma_1 = \sigma_3 + \sigma_d$, the two stress functions are given as:

$$J_1 = \sigma_d + 3\sigma_3 \tag{2}$$

$$J_2/\tau_{oct} = \frac{9\sigma_3^2 + 6\sigma_3\sigma_d}{\sqrt{2}\sigma_d} \tag{3}$$

where

$$J_1 = \sigma_1 + \sigma_2 + \sigma_3$$

$$J_2 = \sigma_1\sigma_2 + \sigma_2\sigma_3 + \sigma_1\sigma_3$$

$$\tau_{oct} = \tfrac{1}{2}[(\sigma_1-\sigma_2)^2 + (\sigma_2-\sigma_3)^2 + (\sigma_1-\sigma_3)^2]^{1/2}.$$

See Cole et al. (1981) for details regarding eq 3.

Moisture tension is incorporated in the modulus expression (eq 1) through the term $[(101.36-\psi)/\psi_o]^{A_1}$ where ψ is in kilopascals, ψ_o is a reference stress of 1 kPa, and 101.36 is atmospheric pressure in kilopascals. For soils in which dry unit weight varied significantly, the term γ_d/γ_o entered into the analysis. γ_o is a reference density of 1 Mg/m³.

As in Part 1 of this series (Cole et al. 1986), the frozen state test data were analyzed in terms of the unfrozen water content, W_u, normalized to the total gravimetric water content, W_T. The expressions for W_u are of the form

$$W_u = a(-\theta/\theta_o)^{-b} \tag{4}$$

where W_u is gravimetric water content expressed as a decimal, a and b are regression constants, θ is the temperature in degrees celsius, and θ_0 is a reference temperature of 1°C. The expressions for W_u were obtained using the pulsed Nuclear Magnetic Resonance (NMR) method* (for additional details, see Cole 1984). The Taxiway A base and subbase materials were too coarse for testing in the NMR device, so it was necessary to estimate the constants needed in eq 4. The exponent b is the more important of the two. A value of 0.25, approximately in the middle of the range of typical values, proved suitable, producing values of R^2 = 0.92 in the resilient modulus regression analyses for each soil in the frozen state. No attempt was made to account for the physical characteristics of the soils in the determination.

The range of validity of the frozen state tests is from -5.0° or -8.8°C, depending on soil type, to the completely thawed state. The analysis was accomplished by including a number of data points representing the condition of the material upon thaw. Clearly, problems are encountered with eq 4 if the soil temperature, θ, is set equal to zero. However, this problem vanishes upon the following consideration. As the temperature of the frozen soil increases, it eventually reaches a point below 0°C at which all the soil water is unfrozen. The temperature at which the soil is completely thawed may be very close to 0°C. This is true for fine-grained soils in general. As a consequence of the mathematical formulation, the unfrozen water content term W_u/W_T goes to 1 before the temperature term goes to 0 and the singularity in eq 2 is thus avoided. Temperatures greater than that required to completely thaw the soil are not meaningful in the frozen soil model. Thus, once the soil is completely thawed, the equations given for the thawed state are used. The equations for the frozen state give sensible values for modulus when the temperature term goes to unity. However, the expressions are generally stress-independent, and should be used only for cases where at least some pore ice is present.

Asphalt concrete

The results of the cyclic uniaxial testing of the asphalt concrete were analyzed, for each type of waveform, in terms of temperature, stress and frequency (for the continuous haversine loading). A second-order expression proved adequate to model the temperature dependency of the resilient modulus.

* Personal communication with A. Tice, CRREL 1984.

RESULTS AND DISCUSSION

General

Appendix B gives a tabulation of all the laboratory test results on the frozen, thawed and unfrozen soil specimens. The tabulation gives confining and deviator stress levels, resilient axial and radial strains, μ_r, M_r, γ_d, gravimetric moisture content and ψ. Temperature is given for all frozen-state tests.

Table 2 gives the results of the regression analyses for all soils under all test conditions. The asphalt concrete analysis results are also given in Table 2, and the results of the analysis are plotted in Figure 4. These equations produce M_r values in megapascals, provided the units of all variables are appropriate (see notes, Table 2). Two or more equations appear for a given soil and state in Table 2. This was done to demonstrate the influence of either different stress functions or additional terms (i.e., a density term) on the empirical result. Subsequent work on the verification of these results using a layered elastic analysis (Johnson et al. 1986b) employs the simplest of these equations with the highest R^2 values to represent a given layer.

A change in the procedure used to analyze the frozen-state test data resulted in somewhat different constants in the regression equations for the frozen soils. The frozen state equations given in Table 2 are based solely on data points obtained from frozen specimens. The highest temperatures were in the range of -0.2° to -0.5°C, and strictly speaking these temperatures define the limit of applicability of the equations. The frozen state equations in Table 2 were used in the layered elastic analysis of the test sections.

A subsequent analysis provided a means to extend the range of applicability of the frozen state equations. This analysis incorporated data points from tests performed upon thawing, and thus resulted in regression equations that are valid at temperatures between the limits of the equations in Table 2 and the melting point. These equations are given in Table 3.

The equations in Table 2 appear somewhat different from the form given in eq 1. The aggregation of all terms other than the stress function raised to a power is to be considered as the term k_1 in eq 1. For the thawed soils, then, k_1 is a function

Table 2. Results of regression analyses—asphalt concrete and test soils from Albany Airport (the standard error is referenced to the natural log of M_r value).

Material	Load pulse	Regression equation	n	R^2	Std. error	Eq. no.
Taxiway A						
Asphalt/concrete	FWD	$^{\dagger}M_r(\mathrm{MPa}) = 1.84\times10^4 \exp[-3.80\times10^{-2}T - 9.14\times10^{-4}T^2]$	88	0.97	0.19	1
	RPB	$M_r(\mathrm{MPa}) = 1.01\times10^4 \exp[-6.50\times10^{-2}T - 6.50\times10^{-4}T^2]$	93	0.98	0.24	2
	Haversine	$M_r(\mathrm{MPa}) = 1.09\times10^4 \exp[-4.75\times10^{-2}T - 7.81\times10^{-4}T^2]f_{\mathrm{Hz}}^{0.20}$	280	0.97	0.22	3
Thawed base	FWD/RPB	$^{\dagger}M_r(\mathrm{MPa}) = 1.10\times10^4[f(\psi)]^{-2.40} f_2(\sigma)^{0.30}$	222	0.82	0.16	4
		$M_r(\mathrm{MPa}) = 4.44\times10^3[f(\psi)]^{-2.20} f_1(\sigma)^{0.37}$	222	0.82	0.16	5
		$M_r(\mathrm{MPa}) = 3.68\times10^4[f(\psi)]^{-2.15} f_2(\sigma)^{0.30} f(\gamma_d)^{3.44}$	222	0.84	0.16	6
		$M_r(\mathrm{MPa}) = 2.56\times10^4[f(\psi)]^{-1.99} f_1(\sigma)^{0.37} f(\gamma_d)^{2.90}$	222	0.82	0.16	7
Frozen base		$^{\dagger}M_r(\mathrm{MPa}) = 1.89\times10^1(w_u/w_t)^{-4.82}$, $w_u = 3\times10^{-2}(-T)^{-0.25}$, $w_t = 0.075$	78	0.78	0.66	8
Thawed subbase	FWD/RPB	$^{\dagger}M_r(\mathrm{MPa}) = 2.07\times10^7[f(\psi)]^{-3.05} f_2(\sigma)^{0.29}$	149	0.80	0.20	9
		$M_r(\mathrm{MPa}) = 4.35\times10^4[f(\psi)]^{-2.72} f_1(\sigma)^{0.37}$	149	0.80	0.20	10
		$M_r(\mathrm{MPa}) = 1.39\times10^{10}[f(\psi)]^{-3.38} f_2(\sigma)^{0.29} f(\gamma_d)^{-7.00}$	149	0.82	0.20	11
		$M_r(\mathrm{MPa}) = 8.00\times10^8[f(\psi)]^{-2.99} f_1(\sigma)^{0.37} f(\gamma_d)^{-5.55}$	149	0.82	0.19	12
Frozen subbase		$^{\dagger}M_r(\mathrm{MPa}) = 8.18\times10^1(w_u/w_t)^{-4.02}$, $w_u = 3\times10^{-2}(-T)^{-0.25}$, $w_t = 0.055$	53	0.70	0.84	13
Non-frozen	FWD/RPB	$^{\dagger}M_r(\mathrm{MPa}) = 1.34\times10^4[f(\psi)]^{-1.50} f_2(\sigma)^{0.33}$	262	0.80	0.80	14
subgrade		$M_r(\mathrm{MPa}) = 7.73\times10^3[f(\psi)]^{-1.34} f_1(\sigma)^{0.35}$	262	0.78	0.17	15
Taxiway B						
Thawed base/	FWD/RPB	$^{\dagger}M_r(\mathrm{MPa}) = 5.55\times10^{10}[f(\psi)]^{-4.72} f_2(\sigma)^{0.27}$	173	0.69	0.26	16
subbase		$M_r(\mathrm{MPa}) = 9.67\times10^9[f(\psi)]^{-4.36} f_1(\sigma)^{0.36}$	173	0.73	0.24	17
		$M_r(\mathrm{MPa}) = 4.28\times10^6[f(\psi)]^{-3.99} f_2(\sigma)^{0.27} f(\gamma_d)^{8.35}$	173	0.71	0.25	18
		$M_r(\mathrm{MPa}) = 1.56\times10^4[f(\psi)]^{-3.69} f_1(\sigma)^{0.36} f(\gamma_d)^{7.72}$	173	0.74	0.23	19
Frozen base/subbase		$^{\dagger}M_r(\mathrm{MPa}) = 1.00\times10^3(w_u/w_t)^{-2.63}$, $w_u = 3\times10^{-2}(-T)^{-0.22}$, $w_t = 0.05$	92	0.96	0.42	20
Thawed subgrade	FWD/RPB	$^{\dagger}M_r(\mathrm{MPa}) = 8.76\times10^5 [f(\psi)]^{-2.38} f_2(\sigma)^{0.30}$	293	0.72	0.20	21
		$M_r(\mathrm{MPa}) = 3.36\times10^5 [f(\psi)]^{-2.15} f_1(\sigma)^{0.34}$	293	0.68	0.21	22
		$M_r(\mathrm{MPa}) = 3.80\times10^4[f(\psi)]^{-2.36} f_2(\sigma)^{-3.25} f(\gamma_d)^{-3.06}$	293	0.74	0.19	23
		$M_r(\mathrm{MPa}) = 1.35\times10^4[f(\psi)]^{-2.13} f_1(\sigma)^{0.34} f(\gamma_d)^{-3.06}$	293	0.70	0.20	24
Frozen subgrade		$M_r(\mathrm{MPa}) = 2.66(w_u/w_t)^{-1.02} f_2(\sigma)^{0.78}$, $w_u = 3.14\times10^{-2}(-T)^{-0.29}$, $w_t = 0.29$	152	0.82	0.92	25
		$M_r(\mathrm{MPa}) = 2.59(w_u/w_t)^{-0.85} f_1(\sigma)^{0.93}$, $w_u = 3.14\times10^{-2}(-T)^{-0.29}$, $w_t = 0.29$	152	0.84	0.85	26
		$M_r(\mathrm{MPa}) = 3.31\times10^1(w_u/w_t)^{-0.87} f_3(\sigma)^{0.68}$, $w_u = 3.14\times10^{-2}(-T)^{-0.29}$, $w_t = 0.29$	152	0.82	0.92	27
Nonfrozen subgrade		$M_r(\mathrm{MPa}) = 5.16\times10^6 [f(\psi)]^{-2.71} f_2(\sigma)^{0.26}$	278	0.81	0.15	28
		$M_r(\mathrm{MPa}) = 5.48\times10^4[f(\psi)]^{-2.71} f_2(\sigma)^{0.26}$	278	0.72	0.18	29
		$M_r(\mathrm{MPa}) = 2.49\times10^6[f(\psi)]^{-2.73} f_2(\sigma)^{0.26} f(\gamma_d)^{2.07}$	278	0.82	0.14	30

NOTES:

RPB = repeated-load plate-bearing apparatus waveform

FWD = falling-weight deflectometer waveform

$\dagger$ = *equations used in analysis*

n = number of points

R^2 = coefficient of determination

M_r = resilient modulus

$T = \theta/\theta_0$

θ = temperature (°C)

θ_0 = 1°C

f_{Hz} = load waveform frequency (Hz)

$f(\gamma) = (101.36-\omega)/\omega_0$

ω = moisture tension (kPa)

ψ_0 = 1 kPa

$f_1(\sigma) = (J_1/\sigma_0)$

$f_2(\sigma) = (J_2/\tau_{oct})/\sigma_0$

$f_3(\sigma) = \tau_{oct})/\sigma_0$

σ = stress (kPa)

σ_0 = 1 kPa

J_1 = first stress invariant (kPa)

J_2 = second stress invariant (kPa)

τ_{oct} = octahedral shear stress (kPa)

$f(\gamma_d) = \gamma_d/\gamma_0$

γ_d = dry unit weight (Mg/m³)

γ_0 = 1 Mg/m³

w_u = unfrozen water content (decimal)

w_t = total water content (decimal)

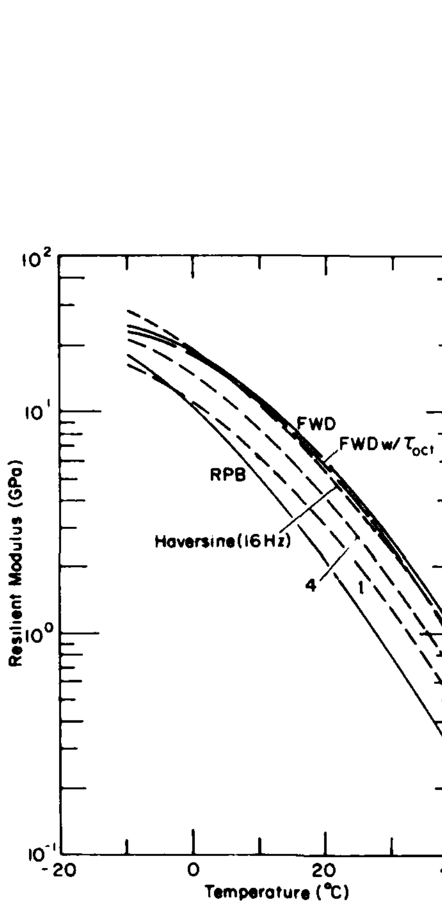

Figure 4. Regression analysis results showing resilient modulus versus temperature for various waveforms for asphalt concrete specimens in repeated load, unconfined compression.

Table 3. Additional regression equations for some frozen soils. The data bases for these equations include points representative of the soils upon thawing.

Material	Load pulse	Regression equation*	n	R^2	Std. error
Taxiway A					
Base, frozen	FWD/RPB	$M_r(\mathrm{MPa}) = 5.80 \times 10^{1} (W_u/WT)^{3.88}$, $W_u = 3 \times 10^{-1}(-T)^{-0.25}$, $WT = 0.075$	104	0.92	0.63
Subbase, frozen	FWD/RPB	$M_r(\mathrm{MPa}) = 6.66 \times 10^{1} (W_u/WT)^{4.68}$, $W_u = 3 \times 10^{-1}(-T)^{-0.25}$, $WT = 0.055$	76	0.92	0.74
Taxiway B					
Subgrade, frozen	FWD/RPB	$M_r(\mathrm{MPa}) = 1.36 \times 10^{2} (W_u/WT)^{-5.26}$, $W_u = 3 \times 10^{-1}(-T)^{0.22}$, $WT = 0.05$	92	0.83	0.89

* See notes of Table 2 for definitions of terms.

Table 4. Average values of resilient Poisson's ratio for the test soils.

	μ_r		μ_r
Taxiway A		**Taxiway B**	
Base	0.33	Base–subbase	0.30
Subbase	0.39	Subgrade	0.35
Subgrade	0.26		

of the term $f(\psi)$, and occasionally a function of dry density through the term $f(\gamma_d)$. The exponent on the $f(\sigma)$ term is, of course, k_2.

As found in Part 1 of this series, the resilient Poisson's ratio, μ_r, was not found to be a systematic function of any of the test variables. Regression analyses similar to those performed for the resilient moduli yielded unacceptably low values of R^2, indicating no clear dependency of μ_r on any of the test variables. Table 4 gives the average values of Poisson's ratio calculated from all the thawed-state test results for each soil.

The regression equations generated the curves given in this section with certain exceptions, noted below.

Resilient modulus

Frozen soil

Figure 5 shows plots of the regression equations for the frozen soils. These equations represent the data rather well: the R^2 values range from 0.83 to 0.92. As can be seen by the form of the equations for the frozen state, the curvature of these relationships is a strong function of the unfrozen water content versus temperature relationship for a particular soil. The modulus of frozen soil can be between two and three orders of magnitude higher than that of the same soil in the thawed state. Some representative data points are also shown in Figure 5. The Taxiway B subgrade was the only soil to exhibit a significant stress dependency. The plotted curve is based on representative values of J_1 for each temperature.

The relatively fine-grained subgrade layers have noticeably lower moduli than the coarse-grained base and subbase layers. The greater unfrozen water content of the fine-grained material undoubtedly contributes substantially to the lower stiffness. Additionally, the Taxiway B subgrade was the only soil to exhibit a systematic stress dependency in the frozen state. The reason for this is unclear. Generally, the stress level effects are so completely overshadowed by the temperature effects that temperature (via the unfrozen water content term) is the only significant variable in the analysis. Inspection of the R^2 values associated with these equations indicates that the inclusion of a stress term only marginally improves the correlation.

As with the soils tested in the earlier phase of this work (Cole et al. 1986), the resilient deformation was not sufficiently large to produce consistently measurable radial deformation in the frozen soil. As a result, we were not able to calculate reliable values for the resilient Poisson's ratio for any of the soils in the frozen state.

Thawed soils

Upon thaw, virtually all test soils developed a moisture tension level of 2.0 kPa, indicating a state of less than complete saturation. As noted above, these soils were tested at several levels of moisture tension up to 24 kPa, which was the highest value recorded in the field test sections.

The dependency of M_r on moisture tension was addressed analytically through the term

$$\left(\frac{101.36-\psi}{\psi_o}\right)^{A_1}$$

The values of A_1 ranged from -1.34 to -4.72 for the Taxiway A subgrade and Taxiway B base–subbase materials respectively. Most values, however, were in the range of -2.2 to -4.0.

The influence of the moisture tension term governs the response of the mathematical model to the thaw recovery phase of the soil. All soils experienced an increase in stiffness with increasing ψ level and the absolute value of the exponent A_1 gives a relative indication of how rapidly the stiffness increases with ψ.

Figure 6 shows the effect of moisture tension level on the term k_1, in eq 1, over the range of 0 to 24 kPa. The curves in Figure 6 were generated from the regression equations and are shown for the k_1 values determined for both stress functions.

As mentioned earlier, and in other work (Cole et al. 1986), the stress function J_2/τ_{oct} proved very effective in representing the stress sensitivity of a number of the test soils. We do not yet have sufficient data to ascertain why certain soils are more favorably represented by this function than by the bulk stress model. Consequently, the stress function that best represents a particular data set is employed in the present work.

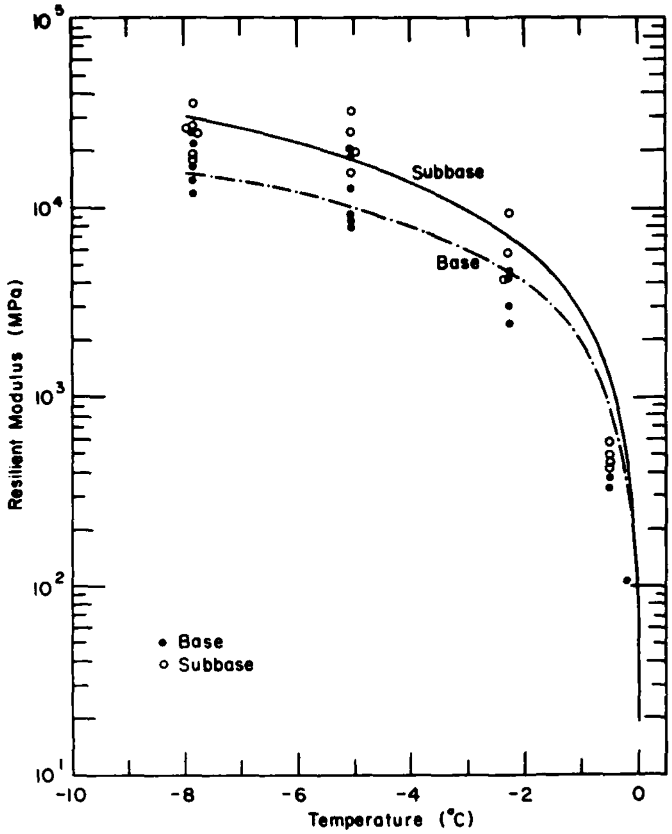

a. Taxiway A soils.

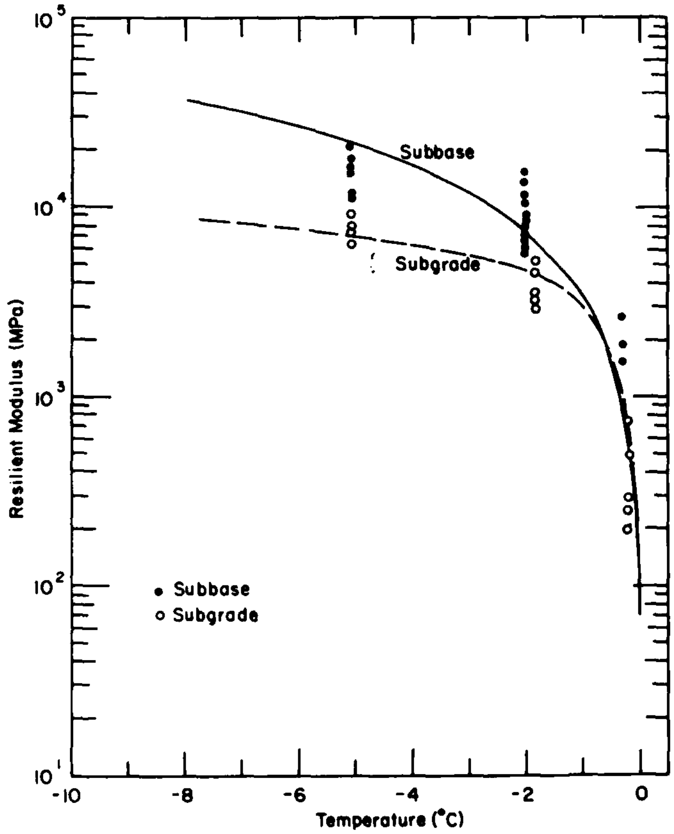

b. Taxiway B soils.

Figure 5. Regression analysis results showing resilient modulus versus temperature.

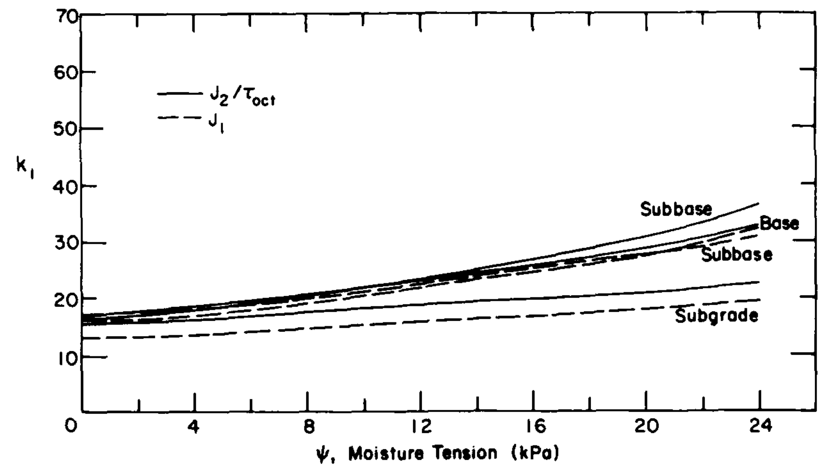

a. Taxiway A.

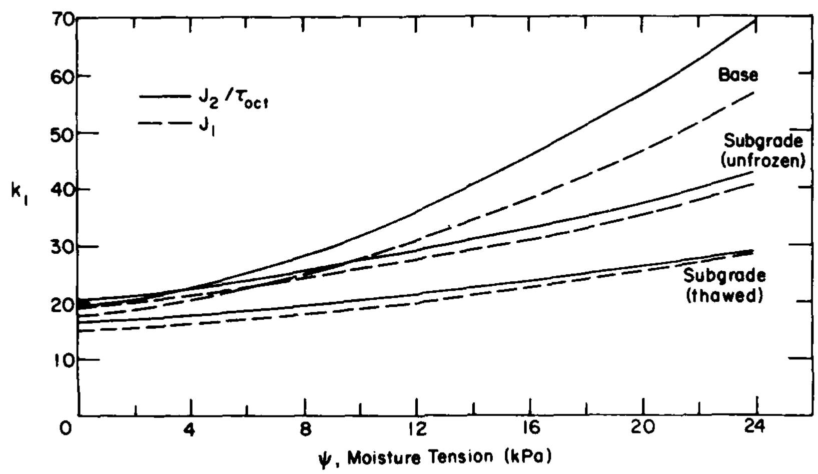

b. Taxiway B.

Figure 6. Dependence on moisture tension of k_1*, the coefficient of either of two stress functions,* J_1 *or* J_2/τ_{oct}*, that characterizes the resilient moduli of thawed and recovering soils.*

Figure 7 shows M_r versus the two stress functions for actual test data from the Taxiway A base layer, ψ = 13.00 kPa. The stress ratio for all test points is indicated. Each grouping of points in Figure 7a corresponds to tests conducted under a constant confining pressure and increasing deviator stress levels. The bulk stress, of course, increases as the deviator stress increases, but the resulting increase in stress ratio brings about a decrease in resilient modulus. This systematic variation of modulus with stress is reduced to virtually random scatter when the data are plotted using the J_2/τ_{oct} stress function as seen in Figure 7b.

The only drawback that we have found to date in using the J_2/τ_{oct} stress function is that it has a singularity when $\tau_{oct} = 0$, i.e., in the case of hydrostatic compression. Under most loading circumstances this would present no problem. However, in the case where the lateral stresses are greater than the vertical stress in the unloaded state, there exists a certain level of applied vertical stress that can, in theory, bring the soil to a hydrostatic stress state and thus cause the denominator in the stress function to go to 0. We are continuing work on this aspect of the analysis with the goal of developing a similar stress function without the singularity problem.

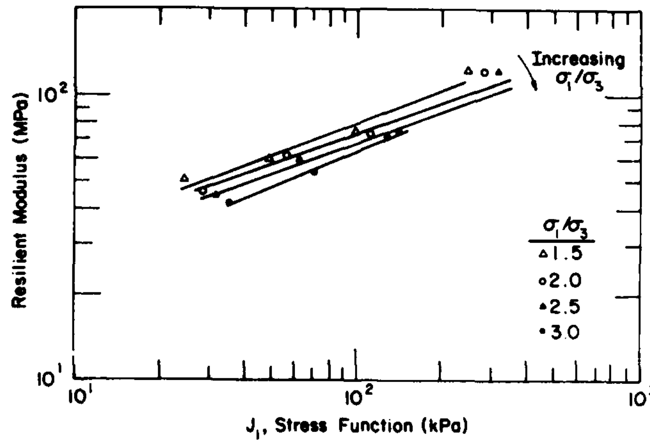

a. J_1.

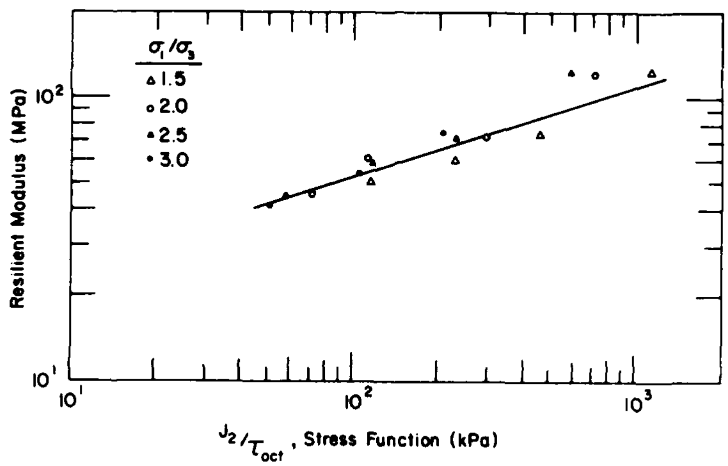

b. J_2/τ_{oct}.

Figure 7. Resilient modulus versus stress functions for several principal stress ratios; actual test data on thawed subgrade from Taxiway B.

Figure 8 shows modulus versus stress function for various levels of moisture tension. The curves were generated by eq 9 and 21, respectively, of Table 2. Note that while the stress function exponents are similar for these two soils, the exponents of the moisture tension level terms differ significantly (3.05 versus -1.5). The fact that the thawed Taxiway A subbase is more sensitive to changes in moisture tension level than the Taxiway A subgrade is evidenced by the wider spacing of the constant moisture tension level curves.

The magnitude of the increase in M_r as a result of natural increases in ψ during thaw recovery varied from a factor of 1.5 to a factor of 3.5 for the Taxiway A subgrade and the Taxiway B base-subbase materials respectively. The dry unit weight, γ_d, varied little through the course of testing. Consequently, a clear dependency of M_r on γ_d does not emerge from these data. Occasionally, as in the case of the thawed Taxiway A base, and the thawed Taxiway B base-subbase, inclusion of a dry unit weight term in the regression analysis improved the correlation coefficient very slightly. The Taxiway B unfrozen subgrade, however, showed a significant improvement in the R^2 value (0.72 to 0.82) by inclusion of the dry unit weight term. Care must be taken in applying the regression equations that contain a γ_d density term. Be-

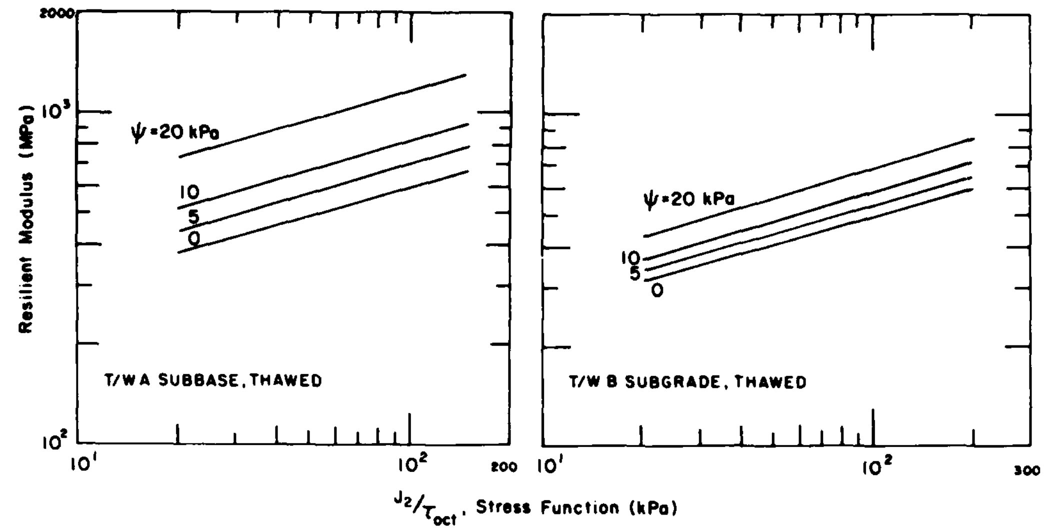

Figure 8. Resilient modulus versus stress function for various levels of moisture tension in the Taxiway A subbase and subgrade (curves on left from eq 9 of Table 2; curves on right from eq 21 of Table 2).

cause the dry unit weights in the SI system of units are close to unity, they can bring about rather large exponents on this term, and substitution of values outside of the range of the data set may result in unrealistic modulus values.

SUMMARY

Frozen- and thawed-soil testing methods and analytical techniques developed in other work (Cole et al. 1986) were applied in a study of frost effects on pavement materials from the Albany County Airport. We developed empirical models of the response of the test soils to cyclic loading in the frozen, thawed and recovered states. The models give resilient modulus as a function of temperature (for soils in the frozen state), stress state, soil moisture tension (for unfrozen soils), and in some cases dry unit weight.

The results of this study are in general agreement with our previous work regarding the effects of temperature, stress level and soil moisture tension level on the resilient modulus. Although we measured Poisson's ratio in all tests, it did not appear to vary systematically with the quantities affecting the resilient modulus, and was thus taken as a constant.

One area of this study indicates that the variations in soil stiffness over a freeze-thaw-recovery cycle can be determined using laboratory test techniques. Another area of this study, reported by Johnson et al. (1986b), verifies the present results using a layered elastic analysis to predict the surface deflections of the Albany County Airport test sections.

CONCLUSIONS

From the foregoing test results and analyses, the following conclusions may be drawn.

1. For the test conditions of this study, the resilient modulus, M_r, of the granular soils tested in the thawed state is well represented by a simple nonlinear model of the form

$$M_r = k_1 f(\sigma)^{k_2}$$

where $f(\sigma) = J_1$ or J_2/τ_{oct}
$k_1 = f(\psi)$, a function of moisture tension
k_2 = constant.

2. The stress function J_2/τ_{oct} was found to adequately reflect the tendency of the granular soils' moduli to increase with increasing confining stress and decrease with increasing principal stress ratio.

3. The increase in stiffness observed subsequent to a freeze-thaw cycle can be expressed through the term k_1, which increases as the soil desaturates.

4. The temperature dependence of the resilient modulus can be expressed through the unfrozen water content:

$$M_r = A_1 \left(\frac{W_u}{W_{ave}}\right)^{A_2}$$

where A_1, A_2 = constants

W_u = unfrozen water content

W_{ave} = total gravimetric water content.

5. Poisson's ratio did not vary systematically with stress or moisture tension level and may consequently be taken as a constant.

6. The variations in soil stiffness throughout a freeze-thaw-recovery cycle can be simulated in the laboratory through the use of open system freezing and proper testing methodology.

LITERATURE CITED

Cole, D.M., L.H. Irwin and T.C. Johnson (1981) Effect of freezing and thawing on resilient modulus of a granular soil exhibiting nonlinear behavior. Transportation Research Board Record 809, pp. 19–26.

Cole, D.M., D. Bentley, G. Durell and T. Johnson (1986) Resilient modulus of freeze-thaw affected granular soils for pavement design and evaluation. Part 1. Laboratory tests on soils from Winchendon, Massachusetts, test sections. USA Cold Regions Research and Engineering Laboratory, Hanover, N.H., CRREL Report 86-4. Also U.S. Department of Transportation, Federal Aviation Administration Report DOT/FAA/PM-84/16,1.

Irwin, L.H. and T.C. Johnson (1981) Frost-affected resilient moduli evaluated with the aid of nondestructively measured pavement surface deflections. Paper presented to the Transportation Research Board task force on nondestructive evaluation of airfield pavements. USA Cold Regions Research and Engineering Laboratory, Hanover, N.H., Internal Report 942 (unpublished).

Johnson, T.C., D.M. Cole and E.J. Chamberlain (1978) Influence of freezing and thawing on the resilient properties of a silt soil beneath an asphalt concrete pavement. USA Cold Regions Research and Engineering Laboratory, Hanover, N.H., CRREL Report 78-23.

Johnson, T.C., D. Bentley and D. Cole (1986a) Resilient modulus of freeze-thaw affected granular soils for pavement design and evaluation. Part 2. Field validation tests at Winchendon, Massachusetts, test sections. USA Cold Regions Research and Engineering Laboratory, Hanover, N.H., CRREL Report 86-12. Also U.S. Department of Transportation, Federal Aviation Administration Report DOT/FAA/PM-84/16,2.

Johnson, T., A. Crowe, M. Erickson and D. Cole (1986b) Resilient modulus of freeze-thaw affected granular soils for pavement design and evaluation. Part 4. Field validation tests at Albany County Airport. USA Cold Regions Research and Engineering Laboratory, Hanover, N.H., CRREL Report 86-13. Also U.S. Department of Transportation, Federal Aviation Administration Report DOT/FAA/PM-84/16,4.

APPENDIX A: SOIL MOISTURE TENSION VERSUS WATER CONTENT FOR SEVERAL TEST SOILS

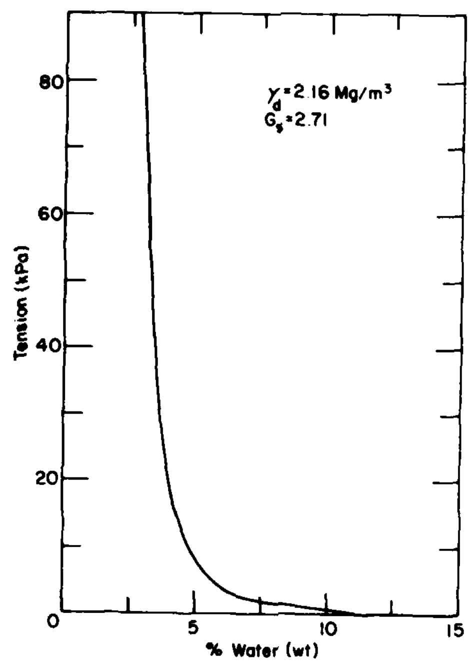

a. Taxiway A base material.

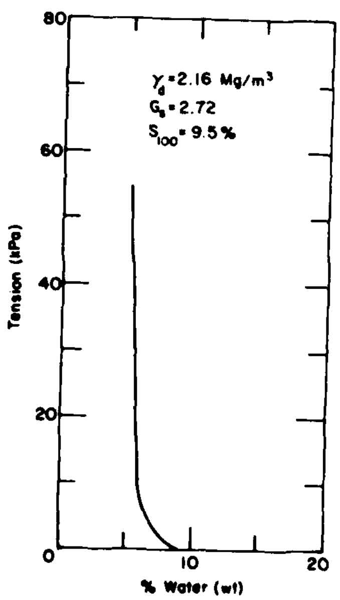

b. Taxiway A subbase material.

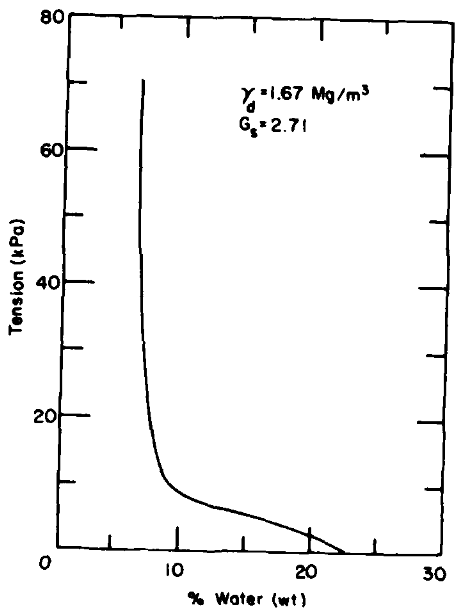

c. Taxiway B subgrade.

Figure A1. Moisture tension versus moisture content.

APPENDIX B: TABULATED RESULTS FOR ALL TESTS ON FROZEN AND THAWED SOILS

Taxiway A

Base layer, frozen

Confining pressure (kPa)	Deviator stress (kPa)	Axial strain $\times 10^{-4}$	Resilient modulus (GPa)	Dry density (Mg/m^3)	Moisture content (%)	Temperature (°C)
69.0	66.9	0.029	23.07	1.890	7.50	-5.0
	136.9	0.064	21.39			
	206.8	0.143	14.46			
	273.7	0.229	11.95			
	340.6	0.343	9.93			
	486.6	0.543	8.96			
	66.9	0.153	4.37	1.890	7.50	-2.2
	136.9	0.325	4.21			
	205.8	0.695	2.96			
	273.7	1.169	2.34			
	66.9	1.569	0.43	1.890	7.50	-0.2
	136.9	3.755	0.36			
27.6	40.1	1.170	0.34			
	53.5	1.532	0.35			
	66.9	1.950	0.34			
69.0	67.5	0.107	6.31	1.932	7.50	-5.0
	138.0	0.257	5.37			
	208.0	0.429	4.85			
	276.0	0.543	5.09			
	344.0	0.686	5.01			
	67.5	0.207	3.26	1.932	7.50	-1.0
	138.0	0.529	2.61			
	208.5	0.886	2.35			
27.6	40.5	0.086	4.71			
	54.0	0.129	4.18			
	67.5	0.214	3.15			
69.0	67.5	0.139	4.85	1.932	7.50	-2.2
	138.0	0.472	2.92			
	208.5	0.750	2.78			
27.6	40.5	0.056	7.23			
	55.2	0.097	5.69			
	67.5	0.139	4.85			
69.0	67.5	0.028	24.10	1.932	7.50	-7.8
	138.0	0.063	21.90			
	208.5	0.139	15.00			
	276.0	0.216	12.78			
	343.5	0.292	11.76			
	490.7	0.445	11.03			
	68.3	0.059	11.58	1.887	7.50	-5.0
	139.8	0.158	8.85			
	211.2	0.290	7.28			
	279.5	0.421	6.64			
	347.9	0.579	6.01			
27.6	68.3	0.056	12.20			
	27.3	0.027	10.12	1.887	7.50	-1.0
	41.0	0.068	6.03			
	54.7	0.108	5.06			
	68.3	0.162	4.22			
69.0	68.3	0.162	4.22			
	139.8	0.676	2.07			
	211.2	1.218	1.73			
	68.3	0.244	2.80	1.887	7.50	-2.2
	139.8	0.623	2.24			
27.6	27.3	0.041	6.67			
	41.0	0.067	6.12			
	54.7	0.122	4.48			
	68.3	0.190	3.60			
69.0	68.4	0.019	36.03	1.887	7.50	-7.8
	1339.8	0.050	267.96			
	211.2	0.125	16.90			
	279.5	0.213	13.12			
	347.9	0.287	12.12			
	496.9	0.500	9.94			
	67.3	0.042	16.04	1.940	7.50	-5.0
	137.8	0.139	9.91			
	208.2	0.208	10.01			
	275.5	0.292	9.43			
	342.9	0.375	9.14			
	489.8	0.583	8.40			
	67.3	0.167	4.03	1.940	7.50	-2.2
	137.8	0.501	2.75			
	208.2	0.891	2.34			
	275.5	1.311	2.10			
27.6	26.9	2.507	0.11	1.940	7.50	-0.2
	13.5	1.253	0.11			
27.6	40.4	3.681	0.11	1.940	7.50	-0.2
69.0	67.3	3.969	0.17			
	137.8	7.990	0.17			

Base layer, thawed

Confining pressure (kPa)	Deviator stress (kPa)	Radial strain $\times 10^{-4}$	Axial strain $\times 10^{-4}$	Resilient Poisson's ratio	Resilient modulus (MPa)	Dry density (Mg/m^3)	Moisture content (%)	Moisture tension (kPa)
6.9	3.4	0.433	0.765	0.475	44.4	1.932	7.30	2.0
	6.9	0.721	1.526	0.453	42.5			
	10.3	1.054	2.357	0.447	43.3			
13.8	6.8	0.444	1.061	0.418	64.1			
	14.0	0.847	2.238	0.376	59.2			
	20.6	1.442	3.541	0.407	58.3			
27.6	14.0	0.499	1.594	0.313	87.6			
	27.9	1.054	3.249	0.324	85.9			
6.9	3.4	0.112	0.411	0.273	83.9	1.979	5.40	6.0
	6.9	0.335	0.981	0.341	70.3			
	10.5	0.502	1.582	0.317	66.1			
	14.2	0.782	2.152	0.363	65.6			
	17.2	1.005	2.596	0.387	66.4			
13.8	6.9	0.223	0.728	0.306	94.7			
	14.2	0.532	1.646	0.325	86.[illegible]			
	20.9	0.782	2.469	0.317	84.6			
	28.3	1.340	3.483	0.385	81.3			
	34.5	1.787	4.244	0.421	81.2			
27.6	14.2	0.559	1.140	0.490	124.2			
	28.3	0.894	2.408	0.371	117.6			
	41.9	1.340	3.612	0.371	115.9			
	56.6	2.122	5.072	0.418	111.7			
69.0	34.5	0.559	1.776	0.315	194.1			
	73.9	1.229	3.807	0.323	194.0			
6.9	3.5	0.112	0.253	0.443	136.6	1.988	4.50	13.0
	6.9	0.224	0.570	0.393	121.2			
	10.5	0.391	0.981	0.399	106.9			
	14.2	0.559	1.392	0.402	101.9			
	17.3	0.727	1.772	0.410	97.5			
13.8	6.9	0.224	0.411	0.545	168.1			
	14.2	0.391	1.013	0.386	140.1			
	21.0	0.643	1.772	0.363	118.4			
	28.4	0.895	2.406	0.372	118.0			
	34.5	1.174	2.975	0.395	116.1			
27.6	14.2	0.168	0.855	0.196	166.0			
	28.4	0.447	1.773	0.252	160.1			
	42.0	0.783	2.723	0.288	154.1			
	56.8	1.341	3.800	0.353	149.4			
69.0	34.5	0.335	1.393	0.240	248.0			
	74.0	0.951	3.167	0.300	233.8			
6.9	3.5	0.112	0.323	0.347	107.1	1.993	3.80	24.0
	6.9	0.224	0.647	0.346	106.9			
	10.5	0.336	1.000	0.336	105.0			
	14.2	0.503	1.353	0.372	105.0			
	17.3	0.615	1.706	0.360	101.3			
13.8	6.9	0.168	0.588	0.286	117.6			
	14.2	0.392	1.206	0.325	117.7			
	21.0	0.559	1.765	0.317	118.9			
	28.4	0.783	2.353	0.333	120.7			
	34.6	0.951	2.765	0.344	125.1			
27.6	14.2	0.280	0.702	0.399	202.3			
	28.4	0.615	1.883	0.327	150.8			
	42.0	0.895	2.648	0.338	158.6			
	56.8	1.175	3.646	0.322	155.7			
69.0	34.6	0.503	1.589	0.317	217.6			
	74.1	1.006	3.237	0.311	228.8			
6.9	3.4	0.222	0.500	0.444	68.1	1.887	7.30	2.0
	6.8	0.459	1.112	0.449	61.3			
	10.3	0.944	1.946	0.485	53.1			
	14.0	1.332	2.615	0.509	53.5			
13.8	6.8	0.333	0.890	0.374	76.5			
	14.0	0.722	1.946	0.371	71.6			
	20.7	1.221	2.896	0.422	71.4			
27.6	14.0	0.416	1.336	0.311	104.7			
	28.0	0.944	2.837	0.326	96.6			
6.9	3.5	0.140	0.421	0.333	82.3	1.929	5.40	6.0
	6.9	0.392	0.947	0.414	73.1			
	10.5	0.616	1.527	0.403	68.8			
	14.2	0.896	2.106	0.425	67.5			
	17.3	1.120	2.475	0.453	70.0			
13.8	6.9	0.224	0.737	0.304	94.0			
	14.2	0.560	1.580	0.354	90.0			
	21.0	0.952	2.423	0.393	86.8			
	28.4	1.343	3.266	0.411	67.1			
27.6	14.2	0.336	1.106	0.304	128.6			
27.6	28.4	0.649	2.371	0.354	120.0	1.929	5.40	6.0
	42.1	1.400	3.532	0.396	119.1			
	56.9	2.071	4.748	0.476	119.8			
69.0	34.6	0.560	1.794	0.312	193.0			
	64.9	1.120	3.272	0.342	198.5			
6.9	3.5	0.112	0.343	0.327	101.0	1.925	4.50	13.0
	6.9	0.224	0.844	0.265	82.1			
	10.5	0.392	1.372	0.286	76.6			
	14.2	0.560	1.847	0.303	77.0			
	17.3	0.784	2.217	0.354	78.1			
13.8	6.9	0.166	0.686	0.245	101.0			
	14.2	0.448	1.583	0.283	89.8			
	21.0	0.728	2.217	0.328	94.0			
	28.4	1.007	2.903	0.347	96.0			
	34.6	1.258	3.537	0.368	97.5			
27.6	14.2	0.336	1.056	0.318	134.7			
	28.4	0.672	2.270	0.296	125.3			
	42.1	1.119	3.273	0.342	125.5			
	56.9	1.568	4.224	0.371	134.7			
69.0	34.6	0.564	1.690	0.298	204.9			
	74.2	1.120	3.434	0.326	216.1			

Confining pressure (kPa)	Deviator stress (kPa)	Radial strain x10^{-4}	Axial strain x10^{-4}	Resilient Poisson's ratio	Resilient modulus (MPa)	Dry density (Mg/m^3)	Moisture content (%)	Moisture tension (kPa)
6.9	3.5	-----	0.219	-----	159.0	1.946	3.80	24.0
	7.0	0.014	0.500	0.028	139.3			
	10.6	0.253	0.813	0.311	130.0			
	14.3	0.336	1.156	0.291	123.7			
	17.4	0.449	1.500	0.299	116.1			
13.8	7.0	0.112	0.469	0.239	148.5			
	14.3	0.337	1.000	0.337	143.0			
	21.1	0.449	1.500	0.299	141.0			
	28.6	0.730	2.125	0.344	134.6			
	34.8	0.898	2.688	0.334	129.6			
27.6	14.3	0.281	0.813	0.346	175.9			
	28.6	0.505	1.750	0.289	163.5			
	42.3	0.786	2.563	0.307	165.0			
	57.2	1.291	3.564	0.362	160.5			
69.0	34.8	0.393	1.438	0.273	242.2			
	71.5	0.842	3.064	0.275	233.4			
6.9	3.3	0.220	0.485	0.454	69.0	1.940	7.30	2.0
	6.7	0.550	1.091	0.504	61.4			
	10.2	0.881	1.819	0.484	55.9			
	13.8	1.156	2.427	0.476	56.7			
13.8	6.7	0.330	0.789	0.418	84.9			
	13.8	0.771	1.699	0.454	80.9			
	20.3	1.321	2.731	0.484	74.4			
27.6	13.8	0.495	1.153	0.429	119.3			
	27.5	0.990	2.733	0.362	100.6			
6.9	3.3	0.110	0.485	0.227	69.0	1.959	5.40	6.0
	6.7	0.330	0.970	0.340	69.0			
	10.2	0.495	1.576	0.314	64.5			
	13.8	0.771	2.243	0.344	61.3			
	16.7	0.990	2.667	0.371	62.8			
13.8	20.3	0.771	2.425	0.318	83.8			
	27.5	1.211	3.457	0.350	79.5			
27.6	40.6	1.100	3.337	0.330	121.8			
	55.0	1.706	4.675	0.365	117.6			
69.0	33.5	0.358	1.700	0.211	196.9			
	65.8	0.825	3.463	0.238	189.9			
6.9	3.4	0.055	0.333	0.165	101.0	1.974	4.50	13.0
	6.7	0.165	0.694	0.238	96.9			
	10.2	0.276	1.056	0.261	96.7			
	13.8	0.441	1.500	0.294	92.1			
	16.6	0.552	1.834	0.301	91.7			
13.8	6.7	0.110	0.583	0.189	115.4			
	13.8	0.331	1.333	0.248	103.7			
	20.4	0.496	1.889	0.263	108.1			
	27.6	0.772	2.501	0.309	110.5			
	33.6	0.992	3.058	0.324	110.0			
27.6	13.8	0.221	1.001	0.221	138.1			
	27.6	0.496	1.946	0.255	142.0			
	40.8	0.772	2.891	0.267	141.2			
	55.2	1.269	3.894	0.326	141.9			
69.0	33.6	0.331	1.502	0.220	223.8			
	72.0	0.772	3.339	0.231	215.8			
6.9	3.4	0.055	0.250	0.220	134.6	1.974	3.80	24.0
	6.7	0.110	0.500	0.220	134.6			
6.9	10.2	0.165	0.776	0.21[illegible]	131.[illegible]	1.974	3.80	24.0
	13.8	0.331	1.056	0.313	130.[illegible]			
	16.8	0.441	1.333	0.331	126.2			
13.8	6.7	0.110	0.444	0.248	151.5			
	13.8	0.276	0.869	0.31[illegible]	155.5			
	20.4	0.386	1.333	0.29[illegible]	153.2			
	27.6	[illegible]	[illegible]	0.321	146.3			
	33.6	0.772	2.334	0.331	144.1			
27.6	13.8	0.221	0.778	0.284	177.[illegible]			
	27.6	0.436	1.611	[illegible]	171.5			
	40.8	0.772	2.334	0.331	175.[illegible]			
	55.3	1.159	2.89[illegible]	0.401	191.[illegible]			
69.0	33.6	0.386	1.112	0.347	302.5			
	72.1	0.827	2.779	[illegible]	259.4			
6.9	3.5	0.225	[illegible]	0.333	59.6	1.89[illegible]	7.30	2.0
	7.0	0.338	1.354	[illegible]	51.7			
	10.6	0.676	2.161	0.31[illegible]	48.7			
13.8	7.0	0.225	[illegible]	0.225	69.9			
	14.1	0.450	2.065	0.218	66.1			
	21.3	0.901	3.249	0.277	65.4			
27.6	14.4	0.225	1.477	0.152	97.4			
	28.8	0.675	2.957	0.228	97.3			
6.9	3.5	0.113	0.417	0.271	84.1	1.91[illegible]	5.40	6.0
	7.0	0.225	0.893	0.252	78.5			
	10.6	0.394	1.468	0.265	71.6			
	14.4	0.563	2.024	0.276	71.1			
	17.5	0.789	2.501	0.315	70.1			
13.8	7.0	0.169	0.774	0.218	90.6			
	14.4	0.394	1.608	0.245	89.6			
	21.3	0.676	2.501	0.270	85.1			
	28.8	1.070	3.396	0.315	84.8			
	35.1	1.634	4.293	0.381	81.7			
27.6	14.4	0.225	1.312	0.171	109.8			
	28.8	0.620	2.564	0.242	112.4			
	42.6	1.014	3.580	0.283	119.0			
	57.6	1.803	5.075	0.355	113.5			
69.0	35.1	0.394	1.792	0.220	195.7			
	75.1	1.070	3.866	0.275	193.4			
6.9	3.5	0.113	0.363	0.311	97.0	1.930	4.50	13.0
	7.0	0.226	0.754	0.300	93.4			
	10.7	0.395	1.173	0.337	91.1			
	14.5	0.565	1.564	0.361	92.5			
	17.6	0.734	2.011	0.365	87.6			
13.8	7.0	0.198	0.671	0.295	104.9			
	14.5	0.395	1.341	0.295	107.8			
	21.4	0.565	1.956	0.289	109.3			
	29.9	0.903	2.571	0.351	112.5			
	35.2	1.242	3.186	0.390	110.5			

Confining pressure (kPa)	Deviator stress (kPa)	Radial strain x10^{-4}	Axial strain x10^{-4}	Resilient Poisson's ratio	Resilient modulus (MPa)	Dry density (Mg/m^3)	Moisture content (%)	Moisture tension (kPa)
27.6	14.5	0.395	1.118	0.353	129.3			
	28.9	0.846	2.124	0.398	136.2			
	42.8	1.354	3.186	0.425	134.2			
	57.8	1.912	4.195	0.456	137.9			
	35.2	0.790	1.734	0.456	203.1			
	72.3	1.354	3.470	0.390	208.4			
69.0	35.2	0.790	1.734	0.456	203.1			
	72.3	1.354	3.470	0.390	208.4			
6.9	3.5	-----	0.308	-----	114.3	1.930	3.80	24.0
	7.0	0.169	0.672	0.251	104.8			
	10.7	0.282	1.007	0.280	106.2			
	14.5	0.395	1.399	0.282	103.4			
	17.6	0.508	1.735	0.293	101.5			
13.8	7.0	0.169	0.560	0.302	125.8			
	14.5	0.339	1.175	0.289	123.1			
	21.4	0.508	1.791	0.284	119.4			
	28.9	0.677	2.406	0.281	120.2			
	35.2	0.903	2.910	0.310	121.0			
27.6	14.5	0.282	1.007	0.280	143.6			
	28.9	0.565	2.015	0.260	143.5			
	42.8	0.903	2.798	0.323	152.8			
	57.8	1.242	3.750	0.331	154.3			
69.0	35.2	0.452	1.567	0.288	224.7			
	72.3	0.960	3.191	0.301	226.6			

Subbase layer, frozen

Confining pressure (kPa)	Deviator stress (kPa)	Axial strain x10^{-4}	Resilient modulus (GPa)	Dry density (Mg/m^3)	Moisture content (%)	Temperature (°C)
69.0	136.0	0.042	32.38	2.020	7.50	-5.0
	206.0	0.083	24.82			
	272.7	0.139	19.62			
	339.3	0.264	12.85			
	484.8	0.486	9.98			
	136.3	0.139	9.81	2.020	7.50	-2.2
	206.0	0.361	5.71			
	272.7	0.639	4.27			
	339.3	0.973	3.49			
27.6	13.3	1.113	0.12	2.020	7.50	-0.2
	26.7	2.646	0.10			
	40.0	4.184	0.10			
69.0	66.6	6.294	0.11			
	136.3	11.230	0.12			
	205.4	0.250	8.22	2.098	7.50	-1.6
	271.8	0.417	6.52			
	337.7	0.584	5.78			
	69.5	0.056	12.40	2.099	7.50	-5.0
	135.9	0.097	14.01			
	205.4	0.139	14.78			
	271.8	0.222	12.24			
	338.2	0.250	13.53			
	483.2	0.361	13.39			
	66.4	0.019	34.97	2.099	7.50	-8.8
	135.9	0.051	26.65			
	205.4	0.077	26.68			
	271.8	0.109	24.94			
	338.3	0.180	18.79			
	483.2	0.295	16.38			
	66.4	0.108	6.15	2.098	7.50	-0.5
	135.7	0.257	5.26			
	205.4	0.405	5.07			
	271.8	0.568	4.79			
	338.3	0.811	4.17			
	136.1	0.042	32.40	2.044	7.50	-5.0
	205.6	0.083	24.77			
	272.2	0.125	21.78			
	338.7	0.181	18.71			
	483.8	0.361	13.40			
	69.5	0.069	10.08	2.044	7.50	-1.4
	136.1	0.153	8.90			
	205.6	0.333	6.17			
	272.2	0.667	4.08			
	338.7	1.001	3.38			
	136.1	0.053	25.68	2.044	7.50	-8.8
	205.6	0.105	19.58			
	272.2	0.158	17.23			
	338.7	0.218	16.13			
	483.8	0.329	14.71			
	136.1	0.184	7.40	2.044	7.50	-0.5
	205.6	0.316	6.51			
	272.2	0.474	5.74			
	338.7	0.684	4.95			

Subbase layer, thawed

Confining pressure (kPa)	Deviator stress (kPa)	Radial strain x10^{-4}	Axial strain x10^{-4}	Resilient Poisson's ratio	Resilient modulus (MPa)	Dry density (Mg/m^3)	Moisture content (%)	Moisture tension (kPa)
6.9	3.3	1.146	0.915	0.599	36.1	2.098	7.50	2.0
	6.6	1.314	1.961	0.670	33.7			
	9.9	2.190	2.943	0.744	33.7			
13.8	6.6	0.766	1.380	0.555	48.0			
	13.3	1.862	2.747	0.678	48.2			
27.6	13.3	0.986	1.731	0.583	77.0			
6.9	3.2	0.161	0.353	0.455	90.5	2.024	6.50	6.0
	6.5	0.463	0.952	0.548	73.6			
	10.0	0.859	1.412	0.608	71.0			
	13.2	1.235	1.942	0.636	68.0			
	17.3	1.826	2.649	0.689	65.3			
13.8	6.6	0.322	0.706	0.456	96.7			
	13.7	0.752	1.589	0.473	86.0			
	20.0	1.181	2.355	0.501	85.1			
	27.3	1.826	3.179	0.574	85.9			
27.6	13.7	0.537	1.119	0.480	122.1			
	27.3	1.128	2.297	0.491	118.9			
6.9	3.4	0.137	0.353	0.383	96.7	2.024	6.00	13.0
	6.8	0.269	0.706	0.381	96.7			
	10.2	0.376	1.059	0.355	96.7			
	13.7	0.591	1.530	0.386	89.3			
	17.1	0.605	2.000	0.402	85.3			
	17.1	0.805	1.941	0.415	87.9			
13.8	6.8	0.215	0.471	0.456	145.0			
	13.7	0.430	1.177	0.365	116.1			
	20.5	0.806	1.883	0.428	108.8			
	27.3	1.181	2.648	0.446	103.2			
27.6	13.7	0.322	0.765	0.421	178.6			
	27.3	0.752	1.883	0.399	145.1			
	41.0	1.449	2.945	0.492	139.1			
	54.6	1.987	4.122	0.482	132.5			
69.0	34.1	0.591	1.472	0.401	231.9			
	68.3	1.235	3.064	0.403	222.9			
6.9	6.8	0.161	0.514	0.313	133.2	2.035	5.50	24.0
	10.3	0.322	0.857	0.376	119.8			
	13.7	0.484	1.200	0.403	114.1			
	17.1	0.645	1.543	0.418	110.9			
13.8	6.8	0.161	0.400	0.402	171.1			
	13.7	0.484	1.200	0.403	114.1			
	20.5	0.645	1.600	0.403	128.3			
	27.4	0.968	2.229	0.434	122.8			
	34.2	1.344	2.972	0.452	115.1			
27.6	13.7	0.269	0.800	0.336	171.1			
	27.4	0.645	1.772	0.364	154.5			
	41.1	1.075	2.743	0.392	149.7			
	54.8	1.612	3.716	0.434	147.4			
69.0	34.2	0.484	1.258	0.385	272.0			
	62.7	0.967	2.744	0.352	228.6			
6.9	3.3	0.327	0.667	0.490	49.1	2.044	7.50	2.0
	6.6	0.762	1.455	0.524	45.1			
	9.8	1.307	2.243	0.583	43.8			
13.8	6.6	0.436	1.273	0.342	51.5			
	13.1	1.089	2.304	0.473	56.9			
	19.7	1.960	3.458	0.567	56.9			
27.6	13.1	0.654	1.577	0.415	83.1			
	26.2	1.525	3.338	0.457	78.6			
6.9	3.3	0.081	0.572	0.142	57.3	2.044	6.50	6.0
	6.6	0.242	1.306	0.185	50.2			
	9.8	0.485	2.041	0.238	48.2			
	13.1	0.647	2.776	0.233	47.2			
13.8	6.6	0.202	0.980	0.206	66.9			
	13.1	0.404	2.042	0.198	64.2			
	19.7	0.687	3.186	0.216	61.7			
27.6	13.1	0.162	1.307	0.124	100.3			
	26.2	0.566	2.860	0.198	91.7			
6.9	3.5	0.109	0.353	0.309	100.1	2.080	6.00	13.0
	6.8	0.219	0.765	0.286	89.3			
	10.6	0.437	1.236	0.354	85.8			
	14.1	0.655	1.648	0.397	85.7			
	17.7	0.874	2.119	0.412	83.3			
13.8	6.8	0.164	0.706	0.232	96.7			
	21.2	0.819	2.119	0.387	100.0			
	28.2	1.201	3.003	0.400	94.0			
27.6	14.1	0.327	1.001	0.327	141.0			
	28.2	0.764	2.179	0.351	129.6			
27.6	42.3	1.256	3.358	0.374	126.1	2.06[illegible]	6.00	13.0
	56.5	1.474	4.716	0.313	119.7			
69.0	32.9	0.546	1.651	0.331	199.5			
	70.6	1.201	3.539	0.339	199.4			
6.9	3.5	-----	0.236	-----	149.5	2.078	5.50	24.0
	6.8	0.218	0.531	0.411	128.5			
	10.6	0.382	0.885	0.432	119.7			
	14.1	0.491	1.190	0.416	119.6			
	17.6	0.546	1.592	0.343	110.8			
13.8	6.8	0.109	0.531	0.205	128.5			
	14.1	0.327	1.062	0.308	132.9			
	21.2	0.601	1.652	0.364	128.1			
	28.2	0.874	2.182	0.401	129.4			
	35.3	0.982	2.714	0.362	130.0			
27.6	14.1	0.273	0.944	0.289	149.5			
	28.2	0.546	1.770	0.308	159.5			
	42.3	0.819	2.655	0.308	159.5			
	56.5	1.366	3.540	0.386	159.5			
69.0	35.3	0.437	1.298	0.337	271.9			
	70.6	0.874	2.951	0.296	239.1			
6.9	3.3	0.220	0.572	0.385	58.3	2.020	7.50	2.0
	6.7	0.550	1.201	0.458	55.6			
	10.1	0.989	2.132	0.464	47.5			

Confining pressure (kPa)	Deviator stress (kPa)	Radial strain x10^{-4}	Axial strain x10^{-4}	Resilient Poisson's ratio	Resilient modulus (MPa)	Dry density (Mg/m^3)	Moisture content (%)	Moisture tension (kPa)
13.8	6.7	0.330	0.948	0.348	70.4			
	13.7	0.879	2.074	0.424	66.1			
	20.3	1.429	3.383	0.464	65.7			
27.6	13.7	0.494	1.482	0.333	92.4			
	27.4	1.154	2.966	0.389	92.4			
	40.5	2.033	4.453	0.457	91.0			
6.9	10.1	0.604	1.143	0.528	88.6	2.020	6.50	6.0
	13.7	0.879	1.714	0.513	80.0			
	16.7	1.209	2.286	0.529	73.0			
13.8	13.7	0.659	1.315	0.501	104.3			
	20.3	0.989	1.829	0.541	110.8			
	27.4	1.539	2.801	0.549	97.9			
	33.4	2.033	3.716	0.547	89.8			
27.6	13.7	0.385	0.915	0.421	149.8			
	27.4	0.879	2.173	0.405	126.1			
	41.7	1.539	3.431	0.449	121.6			
	54.8	2.198	4.577	0.480	119.8			
69.0	33.4	0.550	1.602	0.343	208.3			
	65.5	1.318	3.434	0.384	190.9			
6.9	3.4	0.083	0.342	0.243	99.2	2.065	6.00	13.0
	6.8	0.222	0.737	0.301	92.1			
	10.3	0.388	1.158	0.335	88.9			
	13.9	0.498	1.579	0.315	88.2			
	17.0	0.665	2.000	0.332	84.8			
13.8	6.8	0.111	0.605	0.183	112.2			
	13.9	0.388	1.263	0.307	110.3			
	20.6	0.609	1.895	0.321	108.7			
	27.9	0.887	2.632	0.337	105.9			
	33.9	1.219	3.422	0.356	99.2			
27.6	13.9	0.277	1.000	0.277	139.3			
	27.9	0.664	2.000	0.332	139.3			
	41.2	1.053	3.001	0.351	137.3			
	55.7	1.385	4.055	0.342	137.5			
69.0	33.9	0.610	1.422	0.429	238.6			
	72.7	1.607	3.206	0.501	226.8			
6.9	3.4	0.055	0.211	0.261	160.8	2.069	5.50	24.0
	6.8	0.111	0.474	0.234	143.2			
	10.3	0.222	0.789	0.281	130.5			
	13.9	0.332	1.105	0.300	126.1			
	17.0	0.443	1.421	0.312	119.4			
13.8	6.8	0.111	0.447	0.248	151.8			
	13.9	0.305	1.000	0.305	139.3			
	20.6	0.498	1.526	0.326	135.0			
	27.9	0.720	2.053	0.351	135.8			
	33.9	0.997	2.474	0.403	137.1			
27.6	13.9	0.222	0.842	0.264	165.4			
	27.9	0.665	1.737	0.383	160.4			
	41.2	1.053	2.632	0.400	156.5			
	55.7	1.441	3.422	0.421	162.9			
69.0	33.9	0.498	1.369	0.364	247.8			
	72.7	1.219	3.002	0.406	242.2			

Subgrade layer, thawed

Confining pressure (kPa)	Deviator stress (kPa)	Radial strain x10^{-4}	Axial strain x10^{-4}	Resilient Poisson's ratio	Resilient modulus (MPa)	Dry density (Mg/m^3)	Moisture content (%)	Moisture tension (kPa)
13.8	7.0	0.333	1.056	0.315	66.2	1.650	24.60	2.0
	14.0	0.499	1.961	0.254	71.3			
	20.8	0.999	3.018	0.331	68.8			
	27.3	1.165	4.150	0.281	65.9			
27.6	14.0	0.333	1.434	0.232	97.6			
	27.3	0.832	3.018	0.276	90.6			
	40.4	0.999	4.529	0.221	89.3			
69.0	33.9	0.333	2.264	0.147	149.6			
	70.0	0.999	4.908	0.204	142.5			
	104.9	1.831	7.933	0.231	132.2			
	104.9	1.997	8.311	0.240	126.2			
13.8	14.0	0.499	1.360	0.367	102.9	1.650	22.90	6.0
	21.9	0.832	2.418	0.344	90.4			
	28.4	1.165	3.401	0.343	83.6			
	35.0	1.664	4.309	0.386	81.2			
27.6	28.4	0.832	2.419	0.344	117.5			
	41.5	1.165	3.780	0.308	109.9			
	56.8	1.997	6.050	0.330	94.0			
69.0	35.0	0.499	1.966	0.254	177.9			
	70.0	0.799	4.310	0.232	162.3			
	104.9	2.163	7.945	0.272	132.0			
	139.8	3.659	10.990	0.333	127.2			
13.8	14.0	0.499	1.440	0.347	97.1	1.650	20.70	11.0
	20.8	0.632	2.425	0.343	85.6			
	34.9	1.497	4.395	0.341	79.5			
27.6	28.4	0.665	2.425	0.274	117.1			
	41.5	1.331	4.168	0.319	99.6			
	56.8	1.996	6.064	0.329	93.6			
	69.9	2.661	7.580	0.351	92.2			
69.0	34.9	0.499	1.895	0.263	184.4			
	69.9	0.832	4.548	0.183	153.7			
	104.8	1.996	6.976	0.286	150.2			
	139.8	3.327	10.240	0.325	136.5			
13.8	14.0	0.333	1.062	0.314	131.6	1.650	15.90	21.0
	21.8	0.665	1.669	0.398	130.9			
	28.4	0.832	2.276	0.366	124.7			
	34.9	0.998	3.035	0.329	115.1			

Confining pressure (kPa)	Deviator stress (kPa)	Radial strain $\times 10^{-4}$	Axial strain $\times 10^{-4}$	Resilient Poisson's ratio	Resilient modulus (MPa)	Dry density (Mg/m^3)	Moisture content (%)	Moisture tension (kPa)
27.6	28.4	0.665	1.821	0.365	155.9			
	41.5	0.998	3.035	0.329	136.7			
	56.8	1.331	4.552	0.292	124.7			
	69.9	1.830	5.690	0.322	122.8			
69.0	34.9	0.333	1.821	0.183	191.9			
	69.9	0.832	3.794	0.219	184.2			
	104.8	1.663	6.451	0.258	162.5			
	139.8	2.162	8.349	0.259	167.4			
13.8	14.0	0.333	1.062	0.314	131.6	1.650	14.80	26.0
	21.8	0.499	1.821	0.274	119.9			
	21.8	0.499	2.049	0.244	106.6			
	27.3	0.665	2.429	0.274	112.4			
	34.9	0.998	3.036	0.329	115.1			
27.6	28.4	0.499	1.670	0.299	170.0			
	41.5	0.832	3.036	0.274	136.7			
	54.6	1.331	4.327	0.308	126.2			
	69.9	1.497	5.466	0.274	127.9			
	69.9	1.497	6.073	0.247	115.1			
69.0	34.9	0.333	1.670	0.199	209.2			
	69.9	0.832	3.568	0.233	195.9			
	104.8	1.331	6.073	0.219	172.6			
	104.8	1.331	6.453	0.206	162.4			
	139.8	2.162	8.354	0.259	167.3			
6.9	3.5	-----	0.449	-----	78.0	1.650	24.20	3.0
	7.0	-----	1.046	-----	66.9			
	10.5	0.333	1.868	0.178	56.2			
	14.0	0.250	2.617	0.096	53.5			
13.8	14.0	-----	1.869	-----	74.9			
	21.9	0.333	2.991	0.111	73.2			
	21.9	0.333	3.365	0.099	65.0			
	26.3	0.333	4.862	0.068	54.0			
69.0	35.0	-----	2.769	-----	126.4			
	70.0	0.333	5.612	0.059	124.8			
	105.0	1.332	8.234	0.162	127.5			
	105.0	1.499	8.213	0.183	129.0			
6.9	3.5	0.167	0.599	0.279	58.4	1.650	22.10	8.0
	7.0	0.333	1.348	0.247	51.9			
	10.5	0.666	2.246	0.297	46.7			
6.9	14.0	0.716	2.995	[illegible]	46.7	1.65	22.10	8.0
	17.5	1.166	3.594	0.324	48.7			
13.8	7.0	0.250	[illegible]	[illegible]	58.4			
	14.0	[illegible]	2.121	0.215	63.3			
	21.0	0.999	3.519	0.294	62.0			
	28.4	1.332	4.642	0.297	61.3			
	35.0	1.665	5.792	[illegible]	64.9			
27.6	14.0	0.333	1.472	0.176	74.6			
	28.4	0.799	3.523	0.244	80.8			
	41.6	1.332	4.568	0.274	85.4			
	56.9	1.998	6.741	0.296	84.4			
	70.0	2.331	6.241	0.344	85.0			
69.0	70.0	1.166	5.244	0.222	133.5			
	105.0	2.331	7.869	0.296	133.4			
	140.0	3.330	10.530	0.317	133.3			
6.9	3.5	-----	0.450	-----	77.8	1.65	17.50	17.0
	7.0	0.167	1.050	0.159	66.7			
	10.5	0.333	1.650	0.202	63.6			
	14.0	0.500	2.100	0.238	66.7			
	17.5	0.666	2.624	0.254	66.7			
13.8	7.0	0.167	1.050	0.159	66.7			
	14.0	0.500	1.950	0.256	71.8			
	20.8	0.833	2.774	0.300	74.9			
	28.4	1.166	3.749	0.311	75.9			
	35.0	1.332	4.649	0.287	75.3			
27.6	14.0	0.333	1.500	0.222	93.3			
	28.4	0.833	3.149	0.265	90.3			
	41.6	1.166	4.499	0.259	92.4			
	56.9	1.832	5.999	0.305	94.8			
	70.0	2.331	7.274	0.320	96.3			
69.0	35.0	0.500	2.400	0.208	145.9			
	70.0	0.999	4.499	0.222	155.6			
	105.0	1.832	6.751	0.271	155.5			
	140.0	2.831	9.373	0.302	149.4			
	140.0	2.664	9.373	0.284	149.4			
6.9	3.5	-----	0.300	-----	116.7	1.657	14.80	26.0
	7.0	0.167	0.825	0.202	84.9			
	10.5	0.333	1.351	0.246	77.7			
	14.0	0.500	1.801	0.278	77.7			
	17.5	0.666	2.401	0.277	72.9			
13.8	7.0	0.167	0.825	0.202	84.9			
	14.0	0.333	1.651	0.202	84.8			
	20.8	0.666	2.401	0.277	86.6			
	28.4	0.833	3.376	0.247	84.3			
	35.0	1.166	4.128	0.282	84.8			
27.6	14.0	0.333	1.351	0.246	103.6			
	28.4	0.666	2.852	0.234	99.8			
	41.6	0.999	3.903	0.256	106.5			
	56.9	1.499	5.404	0.277	105.3			
	70.0	1.998	6.755	0.296	103.7			
	70.0	1.998	6.755	0.296	103.7			
69.0	105.0	1.665	5.877	0.283	178.7			
	140.0	2.331	8.634	0.270	162.1			
6.9	3.4	0.165	0.588	0.261	58.4	1.650	24.60	2.0
	6.9	0.495	1.469	0.337	46.8			
	10.3	0.825	2.204	0.374	46.7			
	13.7	1.154	2.943	0.392	46.7			
13.8	6.9	0.330	1.030	0.320	66.7			
	13.7	0.659	2.354	0.280	58.3			
	20.4	1.319	3.460	0.381	58.9			
	27.9	1.813	5.013	0.362	55.7			
27.6	13.7	0.495	1.769	0.280	77.6			
	27.9	1.153	3.686	0.313	75.6			
	27.9	1.153	3.686	0.313	75.6			
	41.8	1.648	5.531	0.298	75.6			
	55.7	2.365	7.388	0.401	75.4			

Confining pressure (kPa)	Deviator stress (kPa)	Radial strain x10^{-4}	Axial strain x10^{-4}	Resilient Poisson's ratio	Resilient modulus (MPa)	Dry density (Mg/m^3)	Moisture content (%)	Moisture tension (kPa)
69.0	34.3	0.659	2.586	0.255	132.5			
	68.5	1.318	5.690	0.232	120.4			
	102.8	2.470	8.507	0.290	120.8			
6.9	3.4	0.165	0.444	0.372	77.2	1.650	22.90	6.0
	6.9	0.329	1.257	0.262	54.5			
	10.3	0.824	1.997	0.413	51.5			
	13.7	0.988	2.590	0.381	52.9			
	17.2	1.318	3.137	0.424	55.3			
13.8	13.7	0.659	2.072	0.318	66.1			
13.8	20.3	0.989	2.959	0.334	68.7	1.650	22.90	6.0
	27.6	1.565	4.071	0.355	69.4			
	34.3	1.812	5.161	0.350	66.1			
27.6	27.8	0.824	3.118	0.265	89.6			
	41.8	1.482	4.812	0.308	86.8			
	55.7	2.141	6.313	0.314	81.7			
	68.5	2.964	8.148	0.364	84.1			
69.0	34.3	0.494	2.519	0.196	136.0			
	102.8	1.812	8.151	0.222	126.1			
6.9	3.4	0.165	0.297	0.556	115.4	1.650	18.50	15.0
	6.9	0.247	0.964	0.256	71.1			
	10.3	0.494	1.464	0.333	69.3			
	13.3	0.576	2.077	0.277	63.9			
	16.7	0.659	2.671	0.247	62.5			
13.8	6.9	0.165	0.890	0.185	77.0			
	13.3	0.412	1.632	0.252	81.4			
	19.3	0.659	2.374	0.275	81.2			
	25.7	0.988	3.339	0.296	77.0			
	34.3	1.482	4.230	0.350	81.0			
27.6	13.7	0.329	1.187	0.277	115.4			
	27.8	0.824	2.597	0.317	107.2			
	41.8	1.153	4.081	0.283	102.3			
	55.7	1.647	6.308	0.261	88.3			
	68.5	0.988	4.602	0.215	148.9			
69.0	34.3	0.329	2.375	0.139	144.3			
	68.5	0.988	4.602	0.215	148.9			
	102.8	1.647	7.052	0.234	145.8			
	137.0	2.635	9.281	0.284	147.6			
6.9	6.9	-----	0.594	-----	115.4	1.650	15.70	22.0
	10.3	0.329	1.040	0.316	98.8			
	13.7	0.412	1.337	0.308	102.5			
	17.1	0.659	1.931	0.341	88.7			
13.8	6.9	-----	0.520	-----	131.8			
	13.7	0.329	1.337	0.246	102.5			
	20.3	0.659	2.154	0.306	94.4			
	27.8	0.824	2.971	0.277	93.7			
	34.3	1.153	3.862	0.299	88.7			
27.6	13.7	0.329	1.040	0.316	131.7			
	27.8	0.659	2.154	0.306	129.2			
	41.8	0.988	3.862	0.256	108.1			
	55.7	1.482	5.348	0.277	104.1			
	68.5	1.976	6.462	0.306	106.0			
69.0	34.3	0.329	2.302	0.143	148.8			
	68.5	0.988	4.308	0.229	159.1			
	102.8	1.482	6.092	0.243	168.7			
	137.0	2.470	8.546	0.289	160.3			
	137.0	2.470	8.546	0.289	160.3			
6.9	3.5	-----	0.603	-----	58.2	1.650	25.20	1.0
	7.0	0.333	1.357	0.245	51.7			
	10.5	0.500	2.263	0.221	46.5			
	14.0	0.750	3.018	0.249	46.6			
	17.6	1.001	3.774	0.265	46.5			
13.8	7.0	0.167	1.132	0.148	62.0			
	14.0	0.417	2.264	0.184	62.1			
	20.8	0.834	3.472	0.240	60.1			
	28.5	1.334	4.908	0.272	58.1			
	35.1	1.667	5.666	0.294	61.9			
27.6	14.0	0.333	1.813	0.184	77.4			
	28.5	0.833	3.400	0.245	83.9			
	41.7	1.167	5.062	0.231	82.3			
	57.0	2.000	6.804	0.294	83.8			
	70.2	2.667	8.701	0.307	80.7			
69.0	35.1	0.500	2.800	0.179	125.4			
	70.2	1.167	5.826	0.200	120.5			
	105.3	2.000	8.326	0.240	126.5			
	140.4	3.000	10.980	0.273	127.9			
6.9	3.5	-----	0.606	-----	57.9	1.650	23.30	5.0
	7.0	0.333	1.363	0.244	51.5			
	10.5	0.500	2.424	0.206	43.4			
	13.2	0.667	3.181	0.210	41.4			
	17.5	1.000	3.938	0.254	44.6			
27.6	14.0	0.333	1.667	0.200	84.2			
	28.5	0.667	3.788	0.176	75.3			
	41.7	1.167	5.114	0.228	81.5			
	57.0	1.833	6.439	0.285	88.6			
27.6	70.2	2.333	7.367	0.317	95.3	1.650	23.30	5.0
69.0	35.1	0.500	2.652	0.189	132.4			
	70.2	1.167	5.684	0.205	123.5			
	105.3	1.833	7.959	0.230	132.3			
	140.4	2.667	10.620	0.251	132.2			
6.9	3.5	-----	0.531	-----	66.1	1.650	20.70	11.0
	7.0	0.167	1.213	0.139	57.9			
	10.5	0.333	1.971	0.169	53.4			
	13.2	0.500	2.730	0.183	48.2			
	17.5	0.667	3.564	0.187	49.2			
13.8	7.0	0.167	1.062	0.157	66.1			
	14.0	0.333	2.275	0.146	61.7			
	20.8	0.667	3.412	0.195	61.1			
	26.5	1.000	4.550	0.220	62.7			
27.6	14.0	0.333	1.517	0.220	92.6			
	28.5	0.667	3.412	0.195	83.6			
	41.7	1.000	4.929	0.203	84.6			
	57.0	1.500	6.447	0.233	88.5			

Confining pressure (kPa)	Deviator stress (kPa)	Radial strain x10^{-4}	Axial strain x10^{-4}	Resilient Poisson's ratio	Resilient modulus (MPa)	Dry density (Mg/m^3)	Moisture content (%)	Moisture tension (kPa)
6.9	3.5	-----	0.455	-----	77.1	1.65[illegible]	15.10	25.0
	7.0	-----	0.910	-----	77.1			
	10.5	0.250	1.441	0.173	73.1			
	14.0	0.333	1.972	0.169	71.2			
	17.5	0.417	2.579	0.162	68.0			
13.8	7.0	-----	0.759	-----	92.6			
	14.0	0.333	1.744	0.191	80.5			
	20.8	0.500	2.656	0.188	78.5			
	28.5	0.750	3.604	0.208	79.1			
	35.1	1.000	4.552	0.220	77.1			
27.6	14.0	0.250	1.366	0.183	102.8			
	28.5	0.500	3.035	0.165	94.0			
	41.7	0.833	4.173	0.200	99.9			
	57.0	1.333	5.690	0.234	100.2			
	70.2	1.667	6.831	0.244	102.8			
69.0	35.1	0.417	2.504	0.167	140.2			
	70.2	1.000	4.932	0.203	142.3			
	105.3	1.667	6.831	0.244	154.2			
	140.4	2.167	9.490	0.228	147.9			

Taxiway B

Subbase layer, frozen

Confining pressure (kPa)	Deviator stress (kPa)	Axial strain x10^{-4}	Resilient modulus (GPa)	Dry density (Mg/m^3)	Moisture content (%)	Temperature (°C)
69.0	71.5	0.051	14.01	1.976	5.50	-5.0
	139.8	0.128	10.92			
	211.3	0.192	11.01			
	279.7	0.256	10.93			
	348.0	0.321	10.84			
	497.2	0.346	14.37			
	71.5	0.058	12.32	1.976	5.50	-2.0
	139.8	0.105	13.31			
	211.3	0.186	11.36			
	280.0	0.279	10.04			
	348.0	0.349	9.97			
	497.2	0.535	9.29			
	71.5	0.282	2.53	1.976	5.50	-0.3
	139.8	0.693	2.02			
	211.3	1.155	1.83			
	279.7	1.669	1.68			
27.6	14.3	0.039	3.66			
	28.0	0.116	2.41			
	41.0	0.193	2.13			
	55.9	0.295	1.90			
	68.4	0.372	1.84			
69.0	70.3	0.048	14.65	2.004	5.50	-5.0
	137.8	0.107	12.88			
	208.0	0.167	12.46			
	275.0	0.202	13.61			
	342.5	0.238	14.39			
	48.9	0.321	1.52			
	70.3	0.107	6.57	2.004	5.50	-2.0
	137.6	0.238	5.78			
	208.0	0.333	6.25			
	275.0	0.429	6.41			
	343.0	0.524	6.55			
	489.4	0.691	7.08			
	70.5	0.163	4.32	2.004	5.50	-0.3
	137.6	0.550	2.50			
	208.0	1.126	1.85			
	275.3	1.627	1.69			
27.6	27.5	0.050	5.51			
	41.6	0.081	5.14			
	55.0	0.106	5.19			
	67.3	0.175	3.85			
69.0	69.4	0.036	19.28	1.965	5.50	-5.0
	135.7	0.119	11.40			
	205.1	0.226	9.08			
	271.4	0.286	9.49			
	337.8	0.333	10.14			
	482.5	0.417	11.57			
	69.4	0.119	5.83	1.965	5.50	-2.0
	135.7	0.214	6.34			
	205.1	0.274	7.49			
	271.4	0.321	8.45			
	337.8	0.381	8.87			
	482.5	0.476	10.14			
	69.4	0.286	2.43	1.965	5.50	-0.3
	135.7	0.548	2.48			
	205.1	0.881	2.33			
	271.4	1.311	2.07			
27.6	13.3	0.048	2.76			
	27.1	0.107	2.54			
	41.0	0.167	2.46			
	54.3	0.215	2.52			
	69.4	0.262	2.65			

Subbase layer, thawed

Confining pressure (kPa)	Deviator stress (kPa)	Radial strain $\times 10^{-4}$	Axial strain $\times 10^{-4}$	Resilient Poisson's ratio	Resilient modulus (MPa)	Dry density (Mg/m^3)	Moisture content (%)	Moisture tension (kPa)
6.9	3.5	0.393	0.571	0.688	61.1	2.076	5.50	2.0
	7.0	0.843	1.238	0.681	56.4			
	10.6	1.405	1.905	0.738	55.6			
	14.3	2.021	2.621	0.771	54.6			
13.8	7.0	0.786	1.239	0.634	56.3			
	14.3	1.797	2.383	0.754	60.1			
	21.2	2.694	3.576	0.753	59.2			
27.6	14.3	0.674	1.574	0.428	90.9			
	28.6	1.685	3.101	0.543	92.3			
	42.3	2.357	4.297	0.549	98.5			
6.9	3.5	0.112	0.390	0.287	88.9	2.091	5.10	6.0
	10.5	0.672	1.220	0.551	86.3			
	14.3	1.008	1.757	0.574	81.1			
	17.3	1.344	2.196	0.612	79.0			
13.8	6.9	0.224	0.708	0.316	98.0			
	14.3	0.728	1.415	0.514	100.7			
	21.1	1.289	2.294	0.562	91.6			
	28.5	1.905	3.172	0.601	89.6			
	34.7	2.688	4.247	0.633	81.7			
27.6	14.3	0.504	1.172	0.430	121.6			
	28.5	1.121	2.344	0.478	121.6			
	42.1	1.680	3.516	0.478	119.8			
	57.0	2.352	4.885	0.481	116.7			
69.0	34.7	0.448	1.563	0.287	221.9			
	74.3	1.233	3.666	0.336	202.8			
6.9	3.5	0.084	0.293	0.287	118.6	2.101	4.80	12.0
	6.9	0.224	0.634	0.353	109.6			
	10.5	0.393	1.024	0.384	103.0			
	14.3	0.617	1.463	0.422	97.5			
	17.4	0.841	1.805	0.466	96.2			
13.8	6.9	0.140	0.537	0.261	129.4			
	14.3	0.449	1.171	0.383	121.9			
	21.1	0.729	1.805	0.404	116.8			
	28.5	1.065	2.440	0.436	117.0			
	37.7	1.514	3.171	0.477	119.0			
27.6	14.3	0.280	0.878	0.319	162.5			
	28.5	0.673	1.903	0.354	150.0			
	42.2	1.065	2.684	0.397	157.2			
	57.1	1.570	3.660	0.429	155.9			
69.0	34.7	0.336	1.318	0.255	263.6			
	74.4	1.009	3.076	0.328	242.0			
6.9	3.5	-----	0.225	-----	154.7	2.107	4.70	17.0
	7.0	0.112	0.450	0.249	154.7			
	10.6	0.168	0.750	0.224	140.8			
	14.3	0.281	1.050	0.268	136.1			
	17.4	0.337	1.300	0.259	133.8			
13.8	7.0	0.056	0.400	0.140	174.0			
	14.3	0.168	0.850	0.198	168.1			
	21.1	0.337	1.350	0.250	156.5			
	28.6	0.449	1.800	0.249	158.8			
	34.8	0.617	2.250	0.274	154.7			
27.6	14.3	0.112	0.700	0.160	204.1			
	28.6	0.281	1.400	0.201	204.1			
	42.3	0.505	2.201	0.229	192.0			
	57.2	0.841	3.001	0.280	190.5			
69.0	34.8	0.168	0.950	0.177	366.3			
	74.6	0.505	2.451	0.206	304.2			
6.9	3.4	0.222	0.439	0.506	77.3	2.080	5.50	2.0
	6.8	0.498	0.927	0.537	73.2			
	10.3	0.776	1.464	0.530	70.4			
	13.9	1.108	2.050	0.540	68.0			
13.8	6.8	0.332	0.732	0.454	92.7			
	13.9	0.610	1.563	0.390	89.2			
	2.6	1.274	2.442	0.522	10.6			
27.6	13.9	0.443	1.172	0.378	118.9			
	27.9	1.053	2.541	0.414	109.7			
	41.2	1.995	4.157	0.480	99.1			
6.9	3.4	0.111	0.286	0.388	118.4	2.091	5.10	6.0
	6.8	0.277	0.619	0.447	109.4			
	10.3	0.498	1.000	0.498	102.8			
	13.9	0.720	1.429	0.504	97.3			
	16.9	0.941	1.762	0.534	96.1			
13.8	6.8	0.166	0.500	0.332	135.5			
	13.9	0.498	1.095	0.455	127.0			
	6.6	0.830	1.762	0.471	37.2			
13.8	27.8	1.162	2.382	0.488	116.8	2.091	5.10	6.0
	33.9	1.550	2.954	0.525	114.6			
27.6	13.9	0.332	0.858	0.387	162.1			
	27.8	0.886	1.906	0.465	145.9			
	41.1	1.605	3.098	0.518	132.7			
	55.6	2.435	4.147	0.587	134.1			
69.0	33.8	0.609	1.526	0.399	221.6			
	72.5	1.500	3.577	0.419	202.8			
6.9	3.4	0.055	0.275	0.200	123.1	2.097	4.80	12.0
	6.8	0.222	0.600	0.370	112.8			
	10.3	0.332	0.950	0.349	108.1			
	13.9	0.554	1.350	0.410	103.0			
	16.9	0.720	1.700	0.424	99.5			
13.8	6.8	0.166	0.500	0.332	135.4			
	13.9	0.388	1.150	0.337	120.9			
	20.5	0.609	1.700	0.358	120.9			
	27.8	0.996	2.401	0.415	115.8			
	33.8	1.328	2.851	0.466	118.7			
27.6	13.9	0.222	0.750	0.296	185.3			
	27.8	0.554	1.751	0.316	158.8			
	41.1	0.996	2.602	0.383	157.9			
	55.6	1.606	3.605	0.446	154.3			
69.0	33.8	0.388	1.301	0.298	260.1			
	72.5	1.107	3.103	0.357	233.7			

Confining pressure (kPa)	Deviator stress (kPa)	Radial strain $\times 10^{-4}$	Axial strain $\times 10^{-4}$	Resilient Poisson's ratio	Resilient modulus (MPa)	Dry density (Mg/m^3)	Moisture content (%)	Moisture tension (kPa)
6.9	3.4	0.355	0.200	0.275	169.4	2.098	4.70	17.0
	6.8	0.166	0.500	0.332	135.5			
	10.3	0.249	0.850	0.293	120.9			
	13.9	0.388	1.150	0.337	121.0			
	16.9	0.554	1.400	0.396	121.0			
13.8	6.8	0.111	0.425	0.261	159.4			
	13.9	0.277	0.900	0.308	154.6			
	20.6	0.471	1.400	0.336	146.9			
	27.8	0.720	1.900	0.379	146.5			
	33.9	0.941	2.350	0.400	144.2			
27.6	13.9	0.166	0.700	0.237	198.7			
	27.8	0.443	1.400	0.316	198.8			
	41.1	0.775	2.051	0.378	200.6			
	55.6	1.107	2.751	0.402	202.3			
69.0	33.9	0.277	1.000	0.277	338.8			
	72.6	0.775	2.251	0.344	322.5			
6.9	3.3	0.275	0.564	0.488	59.3	2.092	5.50	2.0
	6.7	0.960	1.334	0.720	50.1			
	10.1	1.210	2.053	0.589	49.4			
	13.7	1.815	2.824	0.643	48.6			
13.8	6.7	0.385	0.822	0.468	81.3			
	13.7	0.824	1.797	0.459	76.4			
	20.3	1.430	2.672	0.535	75.9			
27.6	13.7	0.495	1.131	0.438	121.4			
	27.5	0.990	2.314	0.428	118.7			
	40.6	1.870	3.859	0.485	105.2			
6.9	3.4	0.110	0.300	0.367	112.4	2.125	5.10	6.0
	6.7	0.276	0.675	0.409	99.9			
	10.2	0.552	1.050	0.526	97.5			
	13.8	0.773	1.500	0.515	92.3			
	16.9	1.050	1.850	0.568	91.1			
13.8	6.7	0.221	0.550	0.402	122.6			
	13.8	0.552	1.150	0.480	120.4			
	20.5	0.884	1.751	0.505	116.9			
	27.7	1.215	2.351	0.517	117.8			
	33.7	1.656	3.002	0.552	112.3			
27.6	13.8	0.331	0.826	0.401	167.7			
	27.7	0.718	1.551	0.463	178.6			
	40.9	1.215	2.663	0.467	157.3			
	55.4	1.878	3.756	0.500	147.5			
69.0	33.7	0.552	1.302	0.424	259.0			
	72.3	1.325	3.007	0.441	240.3			
6.9	3.4	0.055	0.244	0.225	138.7	2.137	4.80	12.0
	6.8	0.138	0.537	0.257	126.1			
	10.3	0.277	0.878	0.315	117.0			
	13.9	0.387	1.171	0.330	118.7			
	16.9	0.553	1.561	0.354	108.4			
13.8	6.8	0.138	0.488	0.283	138.7			
	13.9	0.277	1.024	0.271	135.7			
	20.5	0.498	1.512	0.329	135.9			
	27.8	0.719	2.049	0.351	135.7			
13.8	33.8	0.941	2.537	0.371	133.4	2.137	4.80	12.0
27.6	13.9	0.221	0.732	0.302	189.9			
	27.6	0.443	1.560	0.284	178.2			
	41.1	0.775	2.294	0.338	179.1			
	55.6	1.162	3.026	0.384	183.7			
69.0	33.8	0.387	1.171	0.330	289.0			
	72.5	0.996	2.686	0.371	270.[illegible]			
6.9	3.4	0.055	0.195	0.282	174.2	2.146	4.70	17.0
	6.8	0.111	0.439	0.253	154.7			
	10.3	0.166	0.737	0.235	145.8			
	13.9	0.222	0.927	0.239	150.5			
	17.0	0.277	1.171	0.237	145.0			
13.8	6.8	0.055	0.390	0.141	174.2			
	13.9	0.166	0.854	0.194	163.3			
	20.6	0.277	1.317	0.210	156.6			
	27.9	0.388	1.708	0.227	163.3			
	34.0	0.554	2.147	0.258	158.2			
27.6	13.9	0.111	0.683	0.163	204.2			
	27.9	0.277	1.366	0.203	234.2			
	41.2	0.499	2.098	0.238	196.6			
	55.8	0.776	2.782	0.279	200.6			
69.0	34.0	0.277	1.171	0.237	290.0			
	72.8	0.776	2.538	0.306	286.8			

Subgrade layer, frozen

Confining pressure (kPa)	Deviator stress (kPa)	Axial strain $\times 10^{-4}$	Resilient modulus (GPa)	Dry density (Mg/m^3)	Moisture content (%)	Temperature (°C)
13.8	14.0	0.188	0.75	1.339	29.20	-0.2
	20.6	0.313	0.66			
	27.4	0.563	0.49			
	35.0	0.688	0.51			
27.6	14.0	0.250	0.56			
	27.4	0.500	0.55			
	41.6	0.813	0.51			
	54.8	1.126	0.49			
69.0	102.6	0.170	6.04	1.339	29.20	-1.8
	139.7	0.273	5.12			
	174.6	0.375	4.66			
	205.1	0.477	4.30			
	102.6	0.034	30.18	1.339	29.20	-5.0
	139.7	0.085	16.44			

Confining pressure (kPa)	Deviator stress (kPa)	Axial strain $\times 10^{-4}$	Resilient modulus (GPa)	Dry density (Mg/m^3)	Moisture content (%)	Temperature (°C)
69.0	174.6	0.136	12.84			
	205.2	0.170	12.07			
	272.8	0.238	11.46			
6.9	3.6	0.063	0.57	1.331	29.20	-0.2
	7.2	0.219	0.33			
	10.7	0.438	0.24			
	14.3	0.688	0.21			
	17.9	0.844	0.21			
13.8	7.2	0.219	0.33			
	14.3	0.626	0.23			
	21.0	1.032	0.20			
	27.9	1.439	0.19			
	35.0	1.940	0.18			
27.6	14.3	0.501	0.29			
	27.9	1.064	0.26			
	42.5	1.878	0.23			
	55.9	2.568	0.22			
69.0	35.0	1.566	0.23			
	71.6	3.451	0.21			
	35.5	0.050	7.10	1.331	29.20	-1.8
	71.0	0.132	5.38			
	104.2	0.232	4.49			
	141.9	0.397	3.57			
	177.4	0.629	2.82			
	208.5	0.729	2.86			
	277.2	0.820	3.35			
	71.0	0.018	39.43	1.331	29.20	-5.0
	104.2	0.054	19.30			
	141.9	0.143	9.92			
	177.4	0.214	8.29			
	208.5	0.286	7.29			
	277.2	0.357	7.76			
6.9	3.6	0.071	0.50	1.330	29.20	-0.2
	7.1	0.249	0.29			
	10.7	0.498	0.21			
	14.3	0.676	0.21			
	17.8	0.889	0.20			
13.8	7.1	0.249	0.29			
	14.3	0.640	0.22			
	20.9	0.996	0.21			
	27.8	1.423	0.20			
	35.6	1.788	0.20			
27.6	14.3	0.570	0.25			
	27.8	1.140	0.24			
	42.3	1.852	0.23			
	55.6	2.638	0.21			
69.0	35.6	1.640	0.22			
	71.2	3.714	0.19			
	69.8	0.108	6.46	1.330	29.20	-1.8
	102.6	0.161	6.37			
	139.6	0.287	4.86			
	174.6	0.412	4.24			
	205.1	0.502	4.09			
	272.7	0.717	3.80			
	70.2	0.018	39.01	1.330	29.20	-5.0
	103.1	0.053	19.45			
	140.4	0.107	13.12			
	175.5	0.160	10.97			
	206.2	0.213	9.60			
	274.3	0.320	8.57			
	34.7	0.037	9.38	1.318	29.20	-1.8
69.0	69.4	0.074	9.37	1.318	29.20	-1.4
	101.9	0.148	6.89			
	138.7	0.333	4.17			
	173.4	0.444	3.91			
	203.8	0.704	2.89			
	271.0	1.111	2.44			
	69.2	0.037	18.71	1.318	29.20	-4.2
	101.7	0.055	18.49			
	138.5	0.092	15.35			
	173.1	0.129	13.42			
	203.4	0.221	9.20			
	207.4	0.331	6.27			
	34.7	0.228	1.52	1.318	29.20	-0.2
	35.7	0.252	1.42			
	105.0	1.513	0.69			
	142.9	2.235	0.64			
	178.7	3.029	0.59			
	35.6	0.186	1.91			
	70.8	0.056	12.65	1.333	29.20	-1.8
	104.1	0.093	11.19			
	141.7	0.148	9.57			
	177.1	0.259	6.84			
	208.1	0.370	5.62			
	276.7	0.556	4.98			
	78.8	0.018	39.31	1.333	29.20	-4.2
	103.9	0.054	19.24			
	141.5	0.090	15.72			
	176.9	0.126	14.04			
	207.9	0.180	11.55			
	276.4	0.216	12.80			
	35.4	0.144	2.46	1.333	29.20	-0.2
	70.8	0.540	1.31			

Subgrade layer, thawed

Confining pressure (kPa)	Deviator stress (kPa)	Radial strain $\times 10^{-4}$	Axial strain $\times 10^{-4}$	Resilient Poisson's ratio	Resilient modulus (MPa)	Dry density (Mg/m^3)	Moisture content (%)	Moisture tension (kPa)
6.9	3.6	0.252	0.760	0.332	47.1	1.638	23.80	1.0
	7.2	0.505	1.7[illegible]	0.269	40.9			
	10.7	0.926	2.746	0.337	39.1			
13.8	7.2	0.336	1.258	0.267	56.8			
	14.3	0.757	2.749	0.275	52.0			
	21.6	1.514	4.238	0.353	49.0			
27.6	14.3	0.421	1.876	0.224	76.2			
	26.8	1.009	3.833	0.263	70.3			
	41.3	2.186	5.850	0.374	70.6			
69.0	35.7	0.673	2.926	0.230	122.1			
	71.4	1.434	6.175	0.313	115.7			
6.9	3.6	0.169	0.714	0.237	50.8	1.639	16.20	5.0
	7.3	0.339	1.588	0.213	45.7			
	10.9	0.593	2.382	0.249	45.6			
	14.5	1.015	3.497	0.290	41.4			
	17.2	1.185	4.134	0.287	41.6			
13.8	7.2	0.169	1.192	0.142	60.7			
	14.5	0.592	2.385	0.248	60.7			
	20.8	1.015	3.495	0.290	59.5			
	27.1	1.523	5.090	0.299	53.3			
	36.2	2.537	6.776	0.374	53.4			
27.6	14.5	0.423	1.913	0.221	75.6			
	27.1	1.015	3.747	0.271	72.4			
	42.9	1.777	5.903	0.301	72.7			
	56.4	2.706	7.508	0.360	75.2			
69.0	36.1	0.676	2.875	0.235	125.6			
	72.2	1.691	5.914	0.286	122.2			
	103.8	2.706	8.328	0.325	124.6			
6.9	3.6	0.084	0.536	0.157	67.3	1.638	9.30	12.0
	7.2	0.253	1.112	0.228	64.9			
	10.8	0.422	1.840	0.229	58.7			
	14.4	0.675	2.454	0.275	58.7			
	17.1	0.844	2.915	0.290	58.6			
13.8	7.2	0.168	0.844	0.199	85.2			
	14.4	0.506	1.944	0.260	74.0			
	20.7	0.675	3.068	0.220	67.4			
	28.1	1.181	4.141	0.285	67.8			
	35.9	1.517	5.141	0.295	69.9			
27.6	14.4	0.253	1.535	0.165	93.7			
	28.1	0.844	3.223	0.262	87.1			
	42.6	1.349	4.604	0.293	92.6			
	56.1	2.022	6.450	0.313	87.8			
69.0	35.9	0.506	2.611	0.194	137.5			
	71.8	1.349	5.376	0.251	133.6			
	103.2	2.360	7.688	0.307	134.2			
6.9	3.4	-----	0.364	-----	93.6	1.638	6.10	17.0
	6.8	0.169	0.889	0.198	76.6			
	10.9	0.339	1.617	0.210	67.4			
	13.6	0.424	2.182	0.194	62.4			
	17.2	0.678	2.506	0.271	68.8			
13.8	6.8	0.169	0.808	0.209	84.2			
	13.6	0.339	1.778	0.191	76.5			
	20.9	0.593	2.667	0.222	78.3			
	27.2	0.932	3.558	0.262	76.4			
	34.0	1.101	4.366	0.252	77.9			
27.6	13.6	0.254	1.375	0.185	98.9			
	27.2	0.593	2.749	0.216	98.9			
	40.8	1.316	4.204	0.242	97.0			
	55.5	1.524	56662	0.269	98.0			
69.0	34.0	0.339	2.386	0.142	142.4			
	67.9	1.016	4.531	0.224	149.9			
	106.4	2.031	7.448	0.273	142.9			
	140.3	3.386	9.731	0.348	144.2			
6.9	3.6	0.340	0.642	0.530	56.8	1.637	16.20	5.0
	7.3	0.765	1.560	0.490	46.8			
	10.9	1.360	2.571	0.529	42.6			
	14.6	2.038	3.490	0.584	41.8			
	17.3	2.294	4.043	0.567	42.8			
13.8	7.3	0.340	1.103	0.308	66.1			
	14.6	1.019	2.297	0.444	63.5			
	21.0	1.699	3.308	0.514	63.4			
	27.3	2.463	4.596	0.536	59.5			
	36.4	3.660	6.073	0.603	60.0			
27.6	14.6	0.509	1.564	0.325	93.2			
	27.3	1.189	3.128	0.380	87.3			
27.6	41.0	2.207	4.785	0.461	85.6	1.637	16.20	5.0
	55.7	3.225	6.448	0.50[illegible]	85.9			
69.0	36.4	0.764	2.395	0.319	151.9			
	72.6	2.036	5.160	0.395	141.0			
	104.6	3.225	7.380	0.437	141.7			
6.9	3.4	0.256	0.469	0.546	73.5	1.637	9.30	12.0
	6.9	0.341	0.961	0.348	70.3			
	10.6	0.597	1.664	0.359	63.5			
	13.8	0.768	2.219	0.346	62.1			
	17.4	1.022	2.731	0.374	63.9			
13.8	6.9	0.256	0.854	0.300	80.6			
	13.8	0.597	1.792	0.333	76.8			
	21.1	1.022	2.818	0.363	74.9			
	27.5	1.449	3.758	0.386	73.3			
	34.4	1.789	4.614	0.388	74.5			
27.6	13.8	0.426	1.367	0.312	100.6			
	27.5	0.937	2.734	0.343	100.6			
	43.5	1.704	4.446	0.383	98.0			
	55.0	2.386	5.816	0.410	94.6			
6.9	3.5	0.086	0.363	0.237	95.6	1.637	6.10	17.0
	6.9	0.171	0.945	0.181	73.4			
	10.6	0.428	1.591	0.269	66.8			
	13.8	2.986	2.228	1.340	62.2			
	17.5	2.990	2.547	1.174	68.8			

Confining pressure (kPa)	Deviator stress (kPa)	Radial strain x10^{-4}	Axial strain x10^{-4}	Resilient Poisson's ratio	Resilient modulus (MPa)	Dry density (Mg/m^3)	Moisture content (%)	Moisture tension (kPa)
13.8	6.9	0.171	0.819	0.209	84.5			
	13.8	0.598	1.729	0.346	80.0			
	21.2	0.940	2.729	0.344	77.8			
	27.6	1.367	3.457	0.395	80.0			
	34.6	1.537	4.367	0.352	79.1			
27.6	13.8	0.342	1.410	0.243	98.0			
	27.6	0.854	2.911	0.293	95.0			
	41.5	1.367	4.186	0.327	99.1			
	55.3	2.049	5.645	0.363	98.0			
69.0	34.6	0.598	2.367	0.253	146.0			
	69.1	1.452	4.736	0.307	145.9			
	106.0	2.734	7.294	0.375	145.3			
	138.1	3.928	9.496	0.414	145.4			
6.9	7.2	0.506	0.996	0.508	72.3	1.634	23.80	1.0
	10.8	0.760	1.828	0.416	59.0			
	14.4	1.350	2.831	0.477	50.8			
13.8	7.2	0.337	0.832	0.405	86.4			
	14.4	0.843	1.915	0.440	75.1			
	20.7	1.181	2.999	0.394	68.9			
	28.0	2.192	4.508	0.486	62.2			
27.6	14.4	0.506	1.419	0.357	101.2			
	28.0	1.011	2.923	0.346	96.0			
	41.5	2.022	4.853	0.417	85.5			
6.9	3.7	-----	0.332	-----	110.3	1.634	9.30	12.0
	7.3	0.170	0.830	0.205	88.2			
	11.0	0.511	1.494	0.342	73.5			
	14.6	0.766	1.991	0.385	73.5			
	17.4	0.851	2.572	0.331	67.6			
13.8	7.3	0.170	0.788	0.216	92.9			
	14.6	0.510	1.659	0.307	88.2			
	21.0	0.766	2.531	0.303	83.2			
	27.5	1.192	3.320	0.359	82.7			
	36.6	1.703	4.650	0.366	78.7			
27.6	14.6	0.341	1.162	0.293	126.0			
	27.5	0.681	2.492	0.273	110.2			
	41.2	1.277	3.988	0.320	103.3			
	56.0	1.872	5.570	0.336	100.5			
69.0	36.6	0.510	2.162	0.236	169.1			
	73.1	1.361	4.825	0.282	151.6			
	109.7	2.127	7.331	0.290	149.6			
6.9	3.4	0.089	0.490	0.182	69.7	1.634	6.10	17.0
	6.8	0.169	0.899	0.188	75.9			
	10.9	0.340	1.552	0.219	70.4			
	13.6	0.424	1.961	0.216	69.6			
	17.3	0.509	2.533	0.201	68.2			
13.8	6.8	0.085	0.817	0.104	83.5			
	13.6	0.339	1.634	0.207	83.4			
	20.9	0.509	2.533	0.201	82.5			
	28.4	0.848	3.432	0.247	82.7			
	34.1	1.017	4.250	0.239	80.2			
27.6	13.6	0.169	1.308	0.129	104.2			
27.6	27.3	0.509	2.615	0.195	104.2	1.634	6.10	17.0
	40.9	1.017	3.923	0.259	[illegible]			
	56.6	1.272	5.396	0.236	105.2			
69.0	34.1	0.254	1.963	0.129	173.6			
	68.1	0.678	4.253	0.159	160.2			
	104.5	1.357	6.547	0.207	159.6			
	136.3	2.035	2.375	0.057	573.9			
6.9	3.8	0.348	0.666	0.521	57.2	1.625	23.80	1.0
	7.6	1.042	1.733	0.601	44.0			
	11.4	2.428	2.686	0.904	42.4			
13.8	7.6	0.607	1.106	0.549	68.5			
	15.2	1.648	2.688	0.613	56.5			
	22.3	3.115	4.762	0.654	46.7			
27.6	15.1	0.693	1.905	0.364	79.5			
	29.6	1.558	3.814	0.408	77.6			
	44.9	3.805	6.378	0.597	70.4			
69.0	37.8	0.951	2.711	0.351	139.4			
	75.6	2.249	5.593	0.402	135.1			
6.9	3.8	0.173	0.676	0.256	56.2	1.625	13.50	6.0
	7.6	0.780	1.353	0.576	56.1			
	11.4	1.387	2.369	0.585	48.0			
	15.1	2.077	3.390	0.613	44.7			
13.8	7.6	0.346	1.186	0.292	63.9			
	15.1	1.212	2.373	0.511	63.8			
	21.8	1.991	3.561	0.559	61.1			
	28.3	3.285	5.100	0.644	55.5			
27.6	15.1	0.692	1.700	0.407	88.8			
	28.3	1.555	3.400	0.457	83.3			
	44.8	2.766	5.616	0.493	79.8			
	58.8	4.833	7.682	0.629	76.5			
69.0	37.6	0.863	2.561	0.337	146.9			
	75.3	2.070	5.637	0.367	133.5			
	110.4	3.796	8.559	0.444	129.0			
6.9	7.7	0.349	0.747	0.467	102.6	1.625	9.30	12.0
	11.5	0.522	1.337	0.390	85.9			
	15.3	0.871	1.889	0.461	81.1			
	18.2	1.044	2.362	0.442	77.0			
13.8	7.7	0.261	0.630	0.414	121.6			
	15.3	0.610	1.496	0.408	102.4			
	22.5	1.044	2.363	0.442	95.2			
	28.7	1.392	3.310	0.421	86.7			
	38.2	2.087	4.419	0.472	86.5			
27.6	15.3	0.348	1.184	0.294	129.1			
	28.7	0.870	2.525	0.345	113.5			
	45.4	1.740	4.105	0.424	110.6			
	59.7	2.607	5.533	0.471	107.8			
69.0	38.2	0.783	2.055	0.381	185.8			
	76.4	1.739	4.745	0.366	160.9			
	109.8	2.956	7.127	0.415	154.1			
6.9	7.1	0.173	0.465	0.372	153.5	1.625	6.10	17.0
	10.9	0.347	0.968	0.358	113.0			
	14.3	0.521	1.394	0.374	102.4			
	17.1	0.928	1.782	0.521	96.1			

Confining pressure (kPa)	Deviator stress (kPa)	Radial strain x10^{-4}	Axial strain x10^{-4}	Resilient Poisson's ratio	Resilient modulus (MPa)	Dry density (Mg/m^3)	Moisture content (%)	Moisture tension (kPa)
13.8	14.3	0.434	1.240	0.350	115.1			
	21.9	0.781	1.937	0.403	113.0			
	28.5	1.041	2.790	0.373	102.3			
	35.7	1.476	3.565	0.414	100.1			
27.6	14.3	0.347	1.007	0.345	141.7			
	28.5	0.781	2.170	0.360	131.6			
	42.8	1.215	3.565	0.341	120.0			
	54.7	1.909	4.651	0.410	117.5			
69.0	35.6	0.520	1.860	0.280	191.7			
	71.3	1.215	4.341	0.280	164.2			
	109.2	2.515	7.138	0.352	153.0			
6.9	3.8	-----	0.390	-----	98.2	1.530	9.30	12.0
	7.7	0.348	1.041	0.334	73.5			
	11.0	0.522	1.648	0.317	66.8			
	14.4	0.871	2.255	0.386	63.7			
	17.7	1.044	2.776	0.376	63.8			
13.8	7.2	0.261	0.824	0.317	87.0			
	14.3	0.609	1.735	0.351	82.6			
	21.5	0.957	2.689	0.356	80.0			
	28.6	1.391	3.645	0.382	78.6			
	35.8	1.913	4.514	0.424	79.3			
27.6	14.3	0.348	1.389	0.251	103.1			
27.6	28.6	0.956	2.778	0.344	103.1	1.530	9.30	12.0
	44.1	1.564	4.167	0.375	[illegible]			
	54.9	2.260	5.384	0.420	[illegible]			
69.0	35.8	0.509	2.084	0.292	171.8			
	71.6	1.391	4.343	0.320	164.8			
	109.7	2.606	6.954	0.375	157.6			
6.9	3.8	0.173	0.497	0.348	76.3	1.607	23.80	1.0
	7.6	0.433	1.325	0.327	57.2			
	11.4	0.693	1.988	0.349	57.2			
	15.1	1.126	2.986	0.377	50.7			
13.8	7.6	0.173	0.995	0.174	76.1			
	15.1	0.519	2.157	0.241	70.2			
	22.3	1.038	3.322	0.312	67.0			
	29.5	1.385	4.496	0.308	65.7			
27.6	15.1	0.346	1.495	0.231	100.9			
	29.5	0.865	3.331	0.260	88.7			
	44.9	1.817	5.339	0.340	84.1			
69.0	37.8	0.692	2.503	0.276	151.1			
	75.6	1.644	5.851	0.281	129.3			
6.9	7.4	0.343	0.767	0.447	96.8	1.607	13.50	6.0
	11.1	0.514	1.304	0.394	85.4			
	14.8	0.857	1.994	0.430	74.5			
	18.1	1.028	2.379	0.432	76.1			
13.8	14.8	0.600	1.535	0.391	96.7			
	21.8	1.028	2.456	0.419	88.8			
	27.8	1.371	3.226	0.425	86.2			
	37.0	2.054	4.459	0.461	83.1			
27.6	14.8	0.343	1.230	0.279	120.5			
	27.8	0.856	2.460	0.348	113.0			
	44.0	1.541	3.999	0.385	110.0			
	55.5	2.226	5.388	0.413	103.0			
69.0	37.0	0.513	2.001	0.256	185.0			
	74.0	1.370	4.314	0.318	171.6			
	106.3	2.224	6.487	0.343	163.9			
6.9	3.9	0.088	0.368	0.239	105.3	1.607	9.30	12.0
	7.7	0.263	0.818	0.322	94.7			
	11.6	0.525	1.309	0.401	88.8			
	15.5	0.700	1.759	0.398	87.9			
	18.4	0.875	2.128	0.411	86.4			
13.8	7.7	0.175	0.655	0.267	118.2			
	15.5	0.525	1.432	0.367	108.1			
	22.3	0.788	2.291	0.344	97.2			
	29.0	1.312	3.027	0.433	95.8			
	38.7	1.925	4.090	0.471	94.5			
27.6	15.5	0.350	1.146	0.305	135.0			
	29.0	0.700	2.456	0.285	118.1			
	44.7	1.400	3.767	0.372	118.7			
	58.0	2.099	5.079	0.413	114.2			
69.0	37.5	0.525	2.089	0.251	179.3			
	72.5	1.400	4.261	0.329	170.1			
	111.2	2.623	6.564	0.400	169.4			
6.9	3.5	-----	0.337	-----	102.9	1.607	6.10	17.0
	6.9	0.171	0.675	0.253	102.6			
	10.6	0.342	1.181	0.290	89.9			
	13.8	0.342	1.518	0.225	91.2			
	17.1	0.684	1.856	0.369	92.0			
13.8	6.9	0.170	0.675	0.252	102.5			
	13.8	0.342	1.350	0.253	102.5			
	21.2	0.684	2.025	0.338	104.8			
	27.6	0.940	2.700	0.348	102.4			
	34.6	1.281	3.544	0.361	97.5			
27.6	13.8	0.342	1.181	0.290	117.0			
	26.5	0.512	2.194	0.233	120.8			
	42.6	1.025	3.375	0.304	126.3			
	55.2	1.536	4.558	0.337	121.2			
69.0	34.5	0.427	1.941	0.220	177.8			
	69.0	1.024	3.884	0.264	177.8			
	105.9	1.964	6.250	0.314	169.4			

Subgrade layer, unfrozen

Confining pressure (kPa)	Deviator stress (kPa)	Radial strain x10^{-4}	Axial strain x10^{-4}	Resilient Poisson's ratio	Resilient modulus (MPa)	Dry density (Mg/m^3)	Moisture content (%)	Moisture tension (kPa)
6.9	7.1	0.336	0.714	0.471	100.1	1.533	16.10	12.0
	10.7	0.420	1.071	0.392	100.1			
	14.3	0.673	1.643	0.410	87.0			
	17.9	0.841	2.143	0.392	83.3			
13.8	14.3	0.504	1.429	0.353	100.0			
	21.2	0.841	2.429	0.346	87.3			
	27.9	1.345	3.144	0.428	88.8			
	35.7	1.849	4.002	0.462	89.3			
27.6	14.3	0.504	1.072	0.470	133.1			
	27.9	1.008	2.573	0.392	108.3			
	42.4	1.512	3.716	0.407	114.0			
	55.7	1.848	5.004	0.369	111.3			
	71.3	2.687	6.153	0.437	115.6			
69.0	35.6	0.672	1.717	0.391	207.5			
	71.3	1.511	3.865	0.391	184.4			
6.9	3.5	-----	0.296	-----	118.9	1.497	6.80	17.0
	7.0	0.167	0.739	0.226	95.2			
	10.6	0.250	1.109	0.225	95.2			
	14.1	0.333	1.552	0.215	90.7			
	17.2	0.501	1.996	0.251	86.0			
13.8	7.0	-----	0.592	-----	118.9			
	14.1	0.334	1.331	0.251	105.8			
	20.9	0.501	2.219	0.226	94.1			
	28.6	0.835	3.107	0.269	92.0			
27.6	14.1	0.334	1.110	0.301	126.8			
	27.5	0.667	2.294	0.291	119.8			
	41.8	1.168	3.111	0.375	134.3			
69.0	35.2	0.584	1.852	0.315	190.0			
	70.4	1.335	4.154	0.321	169.5			
6.9	7.1	0.336	0.872	0.385	81.8	1.521	14.80	6.0
	10.7	0.504	1.235	0.408	86.6			
	14.3	0.840	2.035	0.413	70.1			
	17.8	1.008	2.689	0.375	66.3			
13.8	7.1	0.336	0.581	0.578	122.7			
	14.3	0.504	1.599	0.315	89.2			
	21.2	1.008	2.617	0.385	80.9			
	27.8	1.512	3.781	0.400	73.7			
	35.6	2.015	4.875	0.413	73.1			
	35.6	2.184	5.019	0.435	71.0			
27.6	14.3	0.420	1.164	0.361	122.5			
	27.8	1.008	2.581	0.391	107.9			
	42.3	1.511	4.075	0.371	103.9			
	55.7	2.519	5.679	0.444	98.1			
69.0	35.6	0.672	1.820	0.369	195.7			
	71.2	1.679	4.225	0.397	168.6			
6.9	3.6	0.168	0.526	0.319	67.7	1.523	26.10	1.0
	7.1	0.504	1.448	0.348	49.2			
	10.7	0.756	2.501	0.302	42.7			
	14.2	1.175	3.686	0.319	38.6			
	17.8	1.678	4.083	0.411	43.5			
13.8	14.2	0.671	2.305	0.291	61.7			
	21.1	1.342	3.689	0.364	57.2			
	27.7	2.011	5.140	0.391	54.0			
27.6	14.2	0.503	1.581	0.318	89.8			
	27.7	1.006	3.295	0.305	84.2			
	42.2	1.844	5.273	0.350	80.0			
	55.4	3.015	7.256	0.416	76.4			
69.0	35.5	0.838	2.309	0.363	153.6			
	70.9	1.843	5.146	0.358	137.9			
27.6	14.0	0.333	1.289	0.258	108.5	1.469	12.30	8.0
13.8	7.1	0.168	1.000	0.168	71.0	1.496	23.80	3.0
	14.2	0.587	2.429	0.242	58.5			
	21.1	1.006	3.858	0.261	54.6			
	27.7	1.508	4.860	0.310	57.1			
	35.5	2.179	6.293	0.346	56.4			
27.6	14.2	0.335	1.645	0.204	86.3			
	27.7	0.838	3.504	0.239	79.1			
	42.1	1.508	5.293	0.285	79.6			
	55.4	2.513	7.159	0.351	77.4			
69.0	35.5	0.587	2.577	0.228	137.6			
	70.9	1.341	5.299	0.253	133.9			
6.9	7.1	0.168	0.672	0.250	105.4	1.496	10.40	12.0
	10.6	0.335	1.045	0.321	101.6			
	14.2	0.502	1.642	0.306	86.2			
	16.8	0.670	2.090	0.321	80.5			
13.8	21.0	0.670	2.359	0.280	88.0	1.496	10.40	12.0
	27.6	1.004	3.286	0.306	84.1			
	35.4	1.339	4.183	0.320	84.5			
27.6	14.1	0.335	1.120	0.299	126.3			
	27.6	0.669	2.340	0.286	115.6			
	42.0	1.004	3.735	0.269	112.4			
	55.3	1.673	5.081	0.329	108.7			
	70.7	2.509	6.728	0.373	105.1			
69.0	35.4	0.586	1.944	0.301	181.9			
	70.7	1.255	4.337	0.289	163.1			
6.9	3.6	-----	0.303	-----	117.4	1.506	9.30	18.0
	7.1	0.168	0.606	0.277	117.4			
13.8	7.1	0.168	0.682	0.246	104.3			
	14.2	0.336	1.440	0.233	98.8			
	21.1	0.671	2.273	0.295	92.9			
	27.8	0.923	3.103	0.297	89.5			
	35.5	1.258	3.942	0.319	90.2			
27.6	14.2	0.336	1.061	0.317	134.0			
	27.8	0.671	2.426	0.277	114.5			
	42.2	1.006	3.487	0.289	121.0			
	55.5	1.509	4.859	0.311	114.3			
	71.0	2.180	6.373	0.342	111.4			
69.0	35.5	0.503	1.897	0.265	187.2			
	71.0	1.090	4.250	0.256	167.1			
6.9	3.5	-----	0.429	-----	81.0	1.456	10.70	12.0

Confining pressure (kPa)	Deviator stress (kPa)	Radial strain $\times 10^{-4}$	Axial strain $\times 10^{-4}$	Resilient Poisson's ratio	Resilient modulus (MPa)	Dry density (Mg/m^3)	Moisture content (%)	Moisture tension (kPa)
	7.0	-----	0.786	-----	88.5			
13.8	7.0	-----	0.714	-----	97.4			
	13.9	0.332	1.715	0.194	81.1			
	20.6	0.584	2.715	0.215	76.0			
	27.2	0.913	3.574	0.255	76.0			
27.6	13.9	0.332	1.215	0.273	114.5			
	27.2	0.664	2.788	0.238	97.4			
	41.3	1.162	4.436	0.262	93.1			
69.0	34.8	0.664	2.147	0.309	161.9			
	69.5	1.660	4.873	0.341	142.7			
6.9	3.5	-----	0.357	-----	98.6	1.474	21.30	4.0
	7.0	0.334	1.000	0.334	70.4			
	10.6	0.500	1.786	0.280	59.1			
	14.1	0.835	2.572	0.325	54.7			
	17.6	1.168	3.431	0.340	51.3			
13.8	7.0	0.250	0.715	0.350	98.4			
	14.1	0.668	1.787	0.374	78.8			
	20.9	1.001	3.003	0.333	69.6			
	27.5	1.502	4.005	0.375	68.6			
	35.2	2.169	5.295	0.410	66.4			
27.6	27.5	1.001	2.647	0.378	103.9			
	41.7	1.668	4.008	0.416	104.0			
	54.9	2.669	5.732	0.466	95.9			
6.9	14.2	1.341	2.649	0.506	53.6	1.489	23.90	3.0
	17.8	1.761	3.384	0.520	52.5			
13.8	7.1	0.335	0.736	0.455	96.5			
	14.2	0.838	1.913	0.438	74.2			
	21.1	1.508	3.091	0.488	68.2			
	27.7	2.010	3.827	0.525	72.4			
	35.5	3.015	5.007	0.602	70.8			
27.6	27.7	1.005	2.504	0.401	110.7			
	42.1	1.843	4.125	0.447	102.1			
	55.4	2.680	5.307	0.505	104.3			
6.9	7.0	0.500	1.172	0.427	60.0	1.477	26.70	2.0
	10.5	0.834	1.859	0.449	56.8			
	14.1	1.335	2.575	0.518	54.6			
13.8	14.1	0.834	1.788	0.466	78.6			
	20.9	1.335	3.006	0.444	69.4			
27.6	27.5	1.168	2.578	0.453	106.6			
	35.2	1.501	3.870	0.388	90.9			
6.9	10.6	0.335	0.811	0.413	131.3	1.505	9.30	18.0
	14.2	0.503	1.032	0.487	137.6			
	17.3	0.671	1.621	0.414	106.8			
13.8	14.2	0.335	1.032	0.325	137.6			
	21.1	0.671	1.843	0.364	114.4			
	27.7	1.006	2.653	0.379	104.6			
	35.5	1.341	3.391	0.395	104.7			
27.6	27.7	0.671	1.919	0.350	144.6			
	42.2	1.174	2.949	0.398	143.0			
27.6	70.9	2.346	5.638	0.418	126.5	1.505	9.30	18.0
69.0	35.5	0.587	1.476	0.396	240.3			
	70.9	1.257	3.395	0.370	209.0			
6.9	3.5	-----	0.290	-----	120.5	1.476	7.10	19.0
	7.0	-----	0.652	-----	107.2			
	10.5	0.166	1.087	0.153	96.4			
13.8	14.0	0.333	1.377	0.242	101.5			
	20.8	0.333	2.174	0.153	95.4			
	27.3	0.666	2.899	0.230	94.2			
	34.9	0.832	3.768	0.221	92.7			
27.6	14.0	0.166	1.304	0.127	107.2			
	28.4	0.666	2.536	0.263	111.9			
	41.5	0.832	4.259	0.205	102.2			
	54.6	1.165	5.075	0.230	107.6			
6.9	3.5	-----	0.468	-----	75.3	1.496	15.10	6.0
	7.1	0.167	1.014	0.165	69.5			
	10.6	0.340	1.561	0.218	67.8			
	14.1	0.501	2.185	0.229	64.5			
	17.6	0.668	2.731	0.245	64.6			
13.8	7.1	0.167	0.936	0.178	75.3			
	14.1	0.334	1.795	0.186	78.6			
	20.9	0.668	2.653	0.252	78.9			
	26.1	1.003	3.590	0.279	72.6			
	35.3	1.337	4.528	0.295	77.9			
27.6	14.1	0.334	1.483	0.225	95.1			
	28.6	0.668	2.967	0.225	96.6			
	28.6	0.501	2.967	0.169	96.6			
	41.9	1.002	4.374	0.229	95.7			
	55.0	1.670	5.859	0.285	93.9			
	70.4	2.505	7.431	0.337	94.8			
69.0	35.2	0.334	2.190	0.153	160.8			
	70.4	1.000	4.382	0.228	160.8			
6.9	3.5	0.167	0.714	0.234	49.5	1.504	26.40	1.0
	7.1	0.335	1.393	0.240	50.8			
	10.6	0.502	2.143	0.234	49.5			
	14.1	0.837	2.859	0.293	49.5			
	17.7	1.171	3.716	0.315	47.6			
13.8	7.1	0.167	1.108	0.151	63.8			
	14.1	0.669	2.216	0.302	63.8			
	21.0	1.003	3.288	0.305	63.8			
	27.6	1.505	4.575	0.329	60.3			
	35.3	2.006	5.721	0.351	61.8			
27.6	14.1	0.334	1.645	0.203	85.9			
	14.1	0.334	1.645	0.203	85.9			
	27.6	0.836	3.218	0.260	85.8			
	41.9	1.338	4.721	0.283	88.9			
	55.1	2.005	6.153	0.326	89.6			
6.9	3.5	-----	0.294	-----	120.5	1.509	10.30	12.0
	7.1	0.168	0.662	0.254	107.1			
	10.6	0.335	1.103	0.304	96.4			
	14.2	0.502	1.618	0.310	87.6			
	17.7	0.670	2.059	0.325	86.1			

Confining pressure (kPa)	Deviator stress (kPa)	Radial strain $x10^{-4}$	Axial strain $x10^{-4}$	Resilient Poisson's ratio	Resilient modulus (MPa)	Dry density (Mg/m^3)	Moisture content (%)	Moisture tension (kPa)
13.8	7.1	0.168	0.588	0.286	120.5			
	14.2	0.335	1.397	0.240	101.5			
	21.0	0.670	2.206	0.304	95.3			
	27.6	0.837	2.795	0.299	98.9			
	35.4	1.172	3.678	0.319	96.2			
27.6	14.2	0.168	1.103	0.152	128.4			
	27.6	0.502	2.207	0.227	125.3			
	42.0	1.004	3.384	0.297	124.2			
	55.3	1.506	4.857	0.310	113.9			
	70.8	2.175	6.331	0.344	111.8			
69.0	35.4	0.335	2.208	0.152	160.1			
	70.7	1.004	4.122	0.244	171.6			
6.9	10.6	0.334	0.716	0.466	147.6	1.503	6.80	17.0
	14.1	0.417	1.146	0.364	122.9			
	17.6	0.417	1.575	0.265	111.8			
13.8	14.1	0.334	1.074	0.311	131.2			
	20.9	0.501	1.648	0.304	126.9			
	28.6	0.835	2.293	0.364	124.7			
	35.2	1.002	3.297	0.304	106.7			
27.6	14.1	0.250	0.788	0.317	178.7			
	27.5	0.667	1.792	0.372	153.4			
	41.8	1.002	3.298	0.304	126.7			
69.0	35.2	0.500	1.580	0.316	222.7	1.503	6.80	17.0
	70.4	1.166	3.880	0.301	181.4			
6.9	7.1	0.168	1.024	0.164	69.3	1.52[illegible]	14.80	6.0
	10.6	0.335	1.571	0.213	67.7			
	14.2	0.587	2.165	0.265	64.5			
	17.7	0.838	2.868	0.292	61.9			
	17.7	0.838	2.868	0.292	61.9			
13.8	7.1	0.168	0.888	0.189	79.9			
	14.2	0.419	1.844	0.227	77.0			
	21.1	0.670	2.731	0.245	77.1			
	27.7	1.005	3.689	0.272	75.1			
	35.5	1.508	4.646	0.325	76.3			
27.6	14.2	0.251	1.296	0.193	109.3			
	27.7	0.670	2.665	0.251	104.0			
	42.1	1.173	4.101	0.286	102.7			
	98.8	1.843	5.607	0.329	176.3			
69.0	35.5	0.503	2.872	0.175	123.5			
	70.9	1.173	4.652	0.252	152.5			
6.9	7.1	0.334	1.143	0.292	61.7	1.517	26.20	1.0
	10.6	0.669	1.714	0.390	61.8			
	14.1	1.003	2.501	0.401	56.5			
	17.6	1.337	3.145	0.425	56.1			
13.8	7.1	0.167	0.929	0.180	76.0			
	14.1	0.501	1.930	0.260	73.2			
	20.9	1.003	2.860	0.351	73.3			
	27.6	1.671	4.005	0.417	68.8			
	35.3	2.339	5.295	0.442	66.6			
27.6	14.1	0.417	1.288	0.324	109.5			
	27.5	1.002	2.719	0.369	101.3			
	41.9	1.671	4.294	0.389	97.5			
	55.0	2.338	5.729	0.408	96.1			
6.9	3.5	-----	0.606	-----	58.3			
	7.1	0.335	1.212	0.276	58.3			
	10.6	0.669	1.895	0.353	55.9			
	14.1	0.858	2.425	0.354	58.3			
	17.6	1.003	3.184	0.315	55.4			
	3.6	-----	0.379	-----	94.2	1.542	10.10	12.0
	7.1	0.168	0.909	0.185	78.5			
	10.7	0.336	1.364	0.246	78.5			
	14.3	0.504	1.742	0.289	82.0			
	17.8	0.672	2.122	0.317	84.1			
13.8	7.1	0.168	0.758	0.222	94.2			
	14.3	0.336	1.516	0.222	94.2			
	21.2	0.588	2.273	0.259	93.2			
	27.9	0.841	3.031	0.277	92.0			
	35.7	1.177	4.093	0.288	87.2			
27.6	14.3	0.336	1.137	0.296	125.6			
	27.9	0.672	2.426	0.277	114.9			
	42.4	1.008	3.866	0.261	109.6			
	55.8	1.345	5.005	0.269	111.4			
	71.4	2.016	6.829	0.295	104.5			
69.0	35.7	0.504	2.200	0.229	162.2			
	71.4	1.008	4.554	0.221	156.7			

A facsimile catalog card in Library of Congress MARC format is reproduced below.

Cole, David M.
Resilient Modulus of Freeze-Thaw Affected Granular Soils for Pavement Design and Evaluation. Part 3: Laboratory tests on soils from Albany County Airport / by David M. Cole, Diane L. Bentley, Glenn D. Durell and Thaddeus C. Johnson. Hanover, N.H.: Cold Regions Research and Engineering Laboratory; Springfield, Va.: available from National Technical Information Service, 1987.
iii, 40 p., illus.; 28 cm. (CRREL Report 87-2.)
Bibliography: p. 15.
1. Airfields. 2. Freezing-thawing. 3. Laboratory tests. 4. Repeated-load triaxial tests. 5. Resilient moduli. 6. Roads. 7. Soil tests. 8. Subgrade soils. I. Bentley, Diane L. II. Durell, Glenn D. III. Johnson, Thaddeus C. IV. United States. Army. Corps of Engineers. V. Cold Regions Research and Engineering Laboratory, Hanover, N.H. VI. Series: CRREL Report 87-2.

☆ U. S. GOVERNMENT PRINTING OFFICE: 1987--700-050--32,077

END

5-87

DTIC